Enhancing autophagy by redox regulation extends lifespan in *Drosophila*

Authors

Claudia Lennicke[1,2], Ivana Bjedov[3], Sebastian Grönke[4], Katja E. Menger[5], Andrew M. James[5], Jorge Iván Castillo-Quan[6], Lucie A. G. van Leeuwen[1,2], Andrea Foley[1,2], Marcela Buricova[1,2], Jennifer Adcott[6], Alex Montoya[1,2], Holger B. Kramer[1,2], Pavel V. Shliaha[1,2], Angela Logan[5], Filipe Cabreiro[2,7], Michael P. Murphy[5], Linda Partridge[4,6]*, Helena M. Cochemé[1,2]*

Affiliations

[1] MRC Laboratory of Medical Sciences, Du Cane Road, London W12 0HS, UK.

[2] Institute of Clinical Sciences, Imperial College London, Hammersmith Hospital Campus, Du Cane Road, London W12 0HS, UK.

[3] UCL Cancer Institute, 72 Huntley Street, London WC1E 6DD, UK.

[4] Max Planck Institute for Biology of Ageing, Joseph Stelzmann Strasse 9b, 50931 Cologne, Germany.

[5] MRC Mitochondrial Biology Unit, University of Cambridge, Cambridge Biomedical Campus, Hills Road, Cambridge CB2 0XY, UK.

[6] Institute of Healthy Ageing and GEE, University College London, Gower Street, London WC1E 6BT, UK.

[7] CECAD Research Cluster, University of Cologne, Joseph Stelzmann Strasse 26, 50931 Cologne, Germany.

* correspondence: linda.partridge@ucl.ac.uk; helena.cocheme@lms.mrc.ac.uk

Abstract

Dysregulation of redox homeostasis has been implicated in the ageing process and the pathology of age-related diseases. To study redox signalling by H_2O_2 *in vivo*, we established a redox-shifted model by manipulating levels of the H_2O_2-degrading enzyme catalase in *Drosophila*. Here we report that ubiquitous over-expression of catalase robustly extends lifespan in flies. As anticipated, these flies were strongly resistant to a range of oxidative stress challenges, but interestingly were sensitive to starvation, which could not be explained by differences in levels of energy reserves. This led us to explore the contribution of autophagy, which is an important mechanism for organismal survival in response to starvation. We show that autophagy is essential for the increased lifespan upon catalase up-regulation, as the survival benefits were completely abolished upon global autophagy knock-down. Furthermore, using a specific redox-inactive knock-in mutant, we highlight the *in vivo* role of a key regulatory cysteine residue in Atg4a, which is required for the lifespan extension in our catalase model. Altogether, these findings confirm the redox regulation of autophagy *in vivo* as an important modulator of longevity.

Introduction

Redox signalling is a fundamental process that impacts a diverse range of biological pathways[1-4]. Redox regulation can operate through the selective post-translational modification (PTM) of redox-sensitive cysteine residues in target proteins[1-4]. Cysteines are typically present in a reduced, thiol state *in vivo* (–SH)[5-8], but can undergo oxidation in response to specific stimuli, including levels of reactive oxygen species (ROS) or changes in the ratios of redox cofactors, such as $NADPH/NADP^+$ and glutathione/glutathione disulfide. The nature of this oxidative PTM will vary according to the physiological context, but typically proceeds via a sulfenic acid (–SOH) intermediate[1-4].

The redox reactivity of a given cysteine will depend on a combination of physical and biochemical properties. For instance, the position of the cysteine within the tertiary protein structure will determine its accessibility to pro-oxidants, and ability to interact with other redox-dependent binding partners. Additionally, the cysteine pK_a will be influenced by adjacent charged amino acid residues and the local cellular environment, which governs its protonation state and therefore susceptibility to oxidative PTM[1-4]. Critically, redox signalling is distinct from irreversible oxidative damage and functions as a reversible 'redox switch' to regulate target proteins. Dysregulation of redox homeostasis has long been implicated in the pathophysiology of many age-related diseases, as well as in the ageing process itself, however the underlying mechanisms remain largely unclear[9,10].

H_2O_2 acts as the major effector of redox signalling, both directly and through intracellular thiol redox relays[11,12]. The oxidative PTMs induced by H_2O_2 lead to specific changes in cellular pathways, including many processes implicated in ageing[13,14]. To study redox signalling by H_2O_2 *in vivo* and explore its involvement in health and longevity, we used the fruit fly *Drosophila* as a model organism, with its tractable lifespan, powerful genetic tools, and strong evolutionary conservation of many central metabolic pathways with mammals[15]. Here we report that inducing an endogenous redox-shift, by manipulating levels of the H_2O_2-degrading enzyme catalase, improves health and robustly extends lifespan in flies, independently of oxidative stress resistance and dietary restriction. We find that the catalase redox-shifted flies are sensitive to starvation, which relies on autophagy as a vital survival mechanism. Importantly, we show that autophagy is essential for the lifespan extension of the catalase up-regulated flies, which is abolished in an autophagy-deficient background. Furthermore, using a redox-inactive knock-in mutant of Atg4a, a major effector of autophagy, we show that the lifespan extension in response to catalase requires a key redox-regulatory cysteine residue, Cys102 in *Drosophila* Atg4a. These findings demonstrate that redox regulation of autophagy can extend lifespan, confirming the importance of redox signalling in ageing and as a potential pro-longevity target.

Results

Catalase over-expression extends lifespan

To explore the role of endogenous redox signalling by H_2O_2 *in vivo*, we used the binary UAS/GAL4 expression system to up-regulate catalase in wild-type (WT) flies. Global up-regulation of catalase under control of the ubiquitous *daughterless* promoter (da-GAL4>UAS-cat) extended the median and maximum lifespan of female flies (typically by ~10-15%; Fig. 1a, Supplementary Table 1). Importantly, for these experiments, we used the *white Dahomey* (w^{Dah}) background, which is a long-lived and outbred WT, hence we are extending healthy lifespan and not rescuing a short-lived defect. Catalase was over-expressed ~5-10-fold at the mRNA level in whole flies (Supplementary Fig. 1a), which led to corresponding increases in catalase protein (Supplementary Figs. 1b,c) and enzymatic activity (Supplementary Fig. 1d). Interestingly, lifespan was not extended in males (Fig. 1a), despite similar catalase over-expression (Supplementary Figs. 1a,b,d). However, interventions such as modulating nutrient-sensing in *Drosophila* often show gender-specific effects on survival in females, that are absent or marginal in males[16]. Furthermore, over-expression of a mitochondria-targeted catalase (da-GAL4>UAS-mito-cat) did not lead to lifespan extension in either females or males (Supplementary Figs. 1e,f), consistent with a previous study[17], suggesting that altered mitochondrial metabolism is not implicated.

The da-GAL4>UAS-cat flies were mildly delayed in eclosing, without affecting the overall proportion of larvae surviving to adulthood (Supplementary Fig. 1g). To exclude developmental effects, we showed that the lifespan extension could be fully recapitulated using the inducible GeneSwitch system, with over-expression from d2 of adulthood onwards (da-GS>UAS-cat ±RU; Fig. 1b and Supplementary Fig. 1a). Varying the dose of the inducer drug RU (50-400 μM) still did not extend lifespan in males and had only marginal further effects on lifespan extension in females (Supplementary Fig. 1h), suggesting that the catalase benefits are already maximal. Over-expressing catalase under the control of an alternative ubiquitous driver (actin5c-GAL4>UAS-cat) also extended lifespan (Supplementary Fig. 1i). Furthermore, catalase-mediated lifespan extension was independent of *Wolbachia* status (Supplementary Figs. 1j,k), which can influence fly longevity and physiology[18,19]. In addition to lifespan extension, the catalase females also exhibited increased healthspan[20], as inferred from their enhanced climbing ability with age (Fig. 1c). To explore effects on age-specific mortality, trajectories derived from the survival curves revealed a shift in the intercept, but not the slope (Fig. 1d), indicating that catalase up-regulation decreased the overall risk of death, rather than slowing its rate of increase with age[21]. Therefore, the catalase over-expressing flies were healthier for longer.

Using the inducible GeneSwitch system showed that induction of catalase from middle-age (d28 and d42) or old-age (d56) was sufficient to extend lifespan (Fig. 1e and Supplementary Fig. 1l),

although not to the full extent from induction at d2. By d56, the –RU control flies had already started dying, yet switching to +RU treatment even at this late stage still enhanced survival. This implies that for full benefits the redox shift needs to occur early in life, yet late-onset still offers protection. The level of catalase up-regulation induced by RU was equivalent at all ages, as were the levels of endogenous catalase in the controls, eliminating any contribution from changes in RU consumption or endogenous catalase expression with age (Supplementary Fig. 1m). We conclude that ubiquitous up-regulation of catalase improves healthspan and extends lifespan in female flies. Interestingly, tissue-specific catalase up-regulation using a range of drivers (e.g. renal tubules, insulin-producing cells, pan-neuronal, intestine, fat body, pan-muscular; Supplementary Figs. 1n-s), did not recapitulate the strong lifespan extension obtained by the ubiquitous drivers, suggesting that catalase is either acting in an untested tissue (or combination of tissues), or alternatively is required at a global, organismal level. The catalase over-expressors were exceptionally resistant to multiple modes of oxidative stress - by exogenous H_2O_2 (Fig. 1f), the redox cycler paraquat both upon feeding (Fig. 1g) and injection (Fig. 1h), as well as hyperoxia (Fig. 1i and Supplementary Fig. 1t). However, this enhanced oxidative stress resistance is unlikely to explain the lifespan extension in females, because catalase over-expression protected males to a similar extent against oxidative stress without increasing longevity.

Catalase-induced lifespan extension is not through dietary restriction (DR)

To explore the mechanism underlying the catalase-mediated lifespan extension, we examined its relationship to DR, which is a robust and evolutionary conserved nutritional intervention known to have health and longevity benefits[22]. We measured the lifespan response of catalase over-expressor females to DR by varying the yeast content (i.e. protein source) in the food, while maintaining the sugar content constant[23]. This generated a typical tent-shaped response (Fig. 2a), with lifespan decreased at very low yeast levels (0.1x), highest under restricted conditions (0.5x), then gradually shortened towards more fully-fed conditions (1.5x). The lifespan of the catalase flies was enhanced relative to controls at all yeast levels (Fig. 2a), while fecundity increased with yeast content throughout the 0.1-1.5x range for both the control and catalase females (Supplementary Fig. 2a). Therefore, the catalase over-expressor females exhibit a normal DR response, and the lifespan extension upon catalase up-regulation is not mediated by the activation of DR pathways.

While the DR experiment revealed improved survival compared to control at a range of yeast concentrations (Fig. 2a), including extremely poor nutritional conditions (0.1x-yeast; Fig. 2b), we unexpectedly observed that the catalase over-expressing females, but not males, were more sensitive than control to complete starvation (Fig. 2c). There was no difference in triacylglyceride (TAG) levels both basally (t=0) and during a starvation time course, either at d7 (Fig. 2d) or d28

142 (Supplementary Fig. 2b). Similarly, the levels of glycogen storage and mobilisation were the same
143 in control and over-expressor females (Fig. 2e). Therefore, the starvation sensitivity of the catalase
144 flies was not due to differences in metabolic energy reserves or their mobilisation.
145
146 **Autophagy is up-regulated and required for the catalase-mediated lifespan extension**
147 Autophagy is a known longevity assurance process, involved in the response to nutritional
148 challenges such as starvation[24-28]. Furthermore, there is evidence for redox-regulation of
149 autophagy[29]. Therefore, we next explored the involvement of autophagy in the differential starvation
150 response and longevity of the catalase flies. To monitor autophagy status, we stained fly midguts
151 with LysoTracker Red to label autophagolysosomes (Fig. 2f). In parallel, we also monitored
152 autophagic flux using the dye CytoID Green, which accumulates when autophagy is blocked[30]
153 (Supplementary Fig. 2c). The number of LysoTracker punctae was significantly increased in the
154 catalase over-expressors (Fig. 2f), without detectable CytoID staining (Supplementary Fig. 2d),
155 indicating that autophagy is induced without blocking flux. Mitophagy levels were unchanged upon
156 catalase up-regulation as inferred from the genetically-encoded mito-QC fluorescent reporter[31]
157 (Supplementary Fig. 2e).
158 To assess autophagy by an orthologous approach, we quantified the levels of Atg8 (LC3 in
159 mammals), a major autophagosome marker, by immunoblotting. The levels of both the unlipidated
160 (Atg8-I) and lipidated (Atg8-II) forms were strongly elevated in the catalase over-expressors
161 (Fig. 2g), confirming that autophagy was induced. Indeed, levels of autophagy are physiologically
162 fine-tuned, with both autophagy inhibition and excessive activation shown to induce starvation
163 sensitivity *in vivo*[32-34]. Furthermore, similarly to the starvation stress assay, the catalase flies were
164 also sensitive to treatment with the autophagy inhibitor chloroquine (Supplementary Fig. 2f).
165 To test the involvement of autophagy in the longevity of the catalase flies, we down-
166 regulated autophagy by RNAi of Atg5 (Supplementary Fig. 2g), which impairs autophagy[32,34]. Atg5
167 knock-down enhanced sensitivity to starvation (Supplementary Fig. 2h), but did not affect the
168 lifespan of control females under fed conditions (da-GS>UAS-Atg5RNAi ±RU; Fig. 2h), consistent
169 with previous reports[34]. Importantly, the lifespan extension by catalase over-expression was
170 abolished in an Atg5-RNAi background (da-GS>UAS-Atg5RNAi+UAS-cat ±RU; Fig. 2i).
171 Therefore, autophagy is required for the enhanced longevity by catalase up-regulation.
172
173 **Redox proteomics of the catalase up-regulated flies reveals an oxidising shift in bulk thiols**
174 Redox regulation of autophagy has been described for Atg4 in the context of starvation-induced
175 ROS production *in vitro*[35]. Atg4 is the only cysteine peptidase amongst the autophagy components,
176 and is essential for autophagosome biogenesis[29]. Atg4 regulates autophagy by processing Atg8 at

177 two critical stages: 1) the initial cleavage of Atg8, mediated by the redox-insensitive catalytic
178 cysteine of Atg4, therefore this first step promoting Atg8 lipidation is redox-independent; and 2) the
179 subsequent redox-dependent de-lipidation of Atg8, which is selectively inactivated upon oxidation
180 of an adjacent redox-regulatory cysteine in Atg4. Under oxidising conditions, lipidated Atg8
181 accumulates due to the redox-mediated suppression of de-conjugation by Atg4, therefore enhancing
182 autophagosome biogenesis and promoting Atg4-mediated autophagy (Fig. 3a).

183 We previously showed that fasting for 24 h is associated with a strong oxidising shift of bulk
184 cysteine residues *in vivo* in *Drosophila*[6]. We therefore hypothesised that the starvation sensitivity of
185 the da-GAL4>UAS-cat females may be attributed to such thiol redox changes. To explore the effects
186 of catalase up-regulation on global thiol redox state, we applied the same redox proteomic technique
187 (oxidative isotope-coded affinity tags, OxICAT)[6] to the catalase over-expressing females. In
188 OxICAT, samples undergo differential labelling of cysteine residues according to their redox status,
189 followed by trypsin proteolysis and enrichment for cysteine-containing peptides, and finally
190 detection by tandem mass spectrometry (Supplementary Fig. 3a). This allows both the identification
191 of redox-responsive cysteine residues, as well as determination of their redox state. The bulk redox
192 state of cysteines in control flies does not change with age, with the majority remaining at ~10-15%
193 oxidised[6]. In contrast, the catalase over-expressors displayed an oxidising shift in cysteine redox
194 state relative to controls with increasing age (Figs. 3b-d, Supplementary Figs. 3b-e, and
195 Supplementary Tables 2-3). This finding is surprising, since we are over-expressing an antioxidant
196 enzyme. Indeed, we confirmed that global ROS levels were decreased upon catalase up-regulation,
197 as inferred from the redox-sensitive fluorescent dye CellROX (Supplementary Figs. 3f,g).
198 Mitochondrial H_2O_2 levels, measured using the *in vivo* mitochondria-targeted ratiometric mass
199 spectrometry probe MitoB[36], were unchanged in the da-GAL4>UAS-cat females compared to UAS-
200 cat/+ controls (Supplementary Fig. 3h), reflecting the fact that this catalase is not mitochondria-
201 targeted.

202 To reconcile catalase up-regulation with the oxidising shift in bulk cysteine redox state, we
203 tested the hypothesis that by quenching cytoplasmic H_2O_2, catalase over-expression blocks
204 physiological H_2O_2-mediated redox signalling that up-regulates other antioxidant systems and redox
205 couples. The Keap1/Nrf2 signalling pathway is an appealing candidate for this process, as it is an
206 oxidative stress response pathway that enhances the expression of multiple redox systems and is
207 known to be redox-regulated in *Drosophila*[37]. To assess this pathway, we used a transgenic reporter
208 for Keap1/Nrf2 activity, gstD-GFP. This pathway was up-regulated with age in controls, but not in
209 the long-lived catalase flies (Fig. 3e), suggesting that catalase over-expression prevented the
210 induction of Keap1/Nrf2 signalling with age, and thus a range of downstream redox processes.
211 Consistent with this finding, total levels of glutathione - an important cellular antioxidant and redox

212 cofactor, whose synthesis is up-regulated by Nrf2 signalling - were decreased in the catalase
213 overexpressors (Fig. 3f). Altogether, we have shown that catalase flies undergo an unexpected global
214 oxidising thiol redox shift with age. This oxidation is consistent with the enhancement of autophagy
215 via redox-regulation of Atg4.
216
217 **Cys102 in Atg4a is required for the redox-mediated lifespan extension**
218 The protein sequence of Atg4a is evolutionarily conserved, with both the catalytic cysteine (Cys98
219 in *Drosophila*) and the adjacent redox-regulatory cysteine (Cys102 in *Drosophila*) present in flies
220 and mammals. This preservation is highlighted by structural modelling of *Drosophila* Atg4a and
221 alignment analysis against human ATG4A (Figs. 4a,b and Supplementary Fig. 4a). To dissect the
222 physiological role of Atg4 redox-regulation *in vivo*, we generated a transgenic knock-in fly line by
223 CRISPR, where the regulatory cysteine in endogenous Atg4a was replaced by a redox-inactive
224 serine residue (C102S mutant). This C102S knock-in mutation did not affect Atg4a expression
225 (Supplementary Fig. 4b), or levels of catalase activity both basally and upon genetic up-regulation
226 (Supplementary Fig. 4c). Catalase over-expression in Atg4a-C102S knock-in flies displayed the
227 same strong resistance to H_2O_2-induced oxidative stress as in the Atg4a-WT background
228 (Supplementary Fig. 4d).
229 Basal levels of autophagy were not affected under control conditions in the redox knock-in
230 line (UAS-cat/+, Atg4a-WT *v.* UAS-cat/+, Atg4a-C102S), whereas autophagy induction by catalase
231 over-expression was abolished (da-GAL4>UAS-cat, Atg4a-C102S), as assessed both by Western
232 blotting against Atg8 (Fig. 4c and Supplementary Fig. 4e) and LysoTracker staining (Fig. 4d and
233 Supplementary Fig. 4f). Therefore, this redox-regulatory cysteine in Atg4a is required for autophagy
234 induction by redox signalling *in vivo*, as previously reported *in vitro*[35].
235 To interrogate the role of Atg4a-Cys102 in mediating the longevity of the catalase flies, we
236 performed survival assays with the Atg4a-WT CRISPR control line, and reproduced the catalase
237 lifespan extension in this background (Fig. 4e). The Atg4a-C102S point mutation did not affect
238 survival of control flies, confirming that this knock-in alone is not deleterious (Fig. 4f). Critically,
239 in contrast to the Atg4a-WT control, the lifespan extension upon catalase up-regulation was fully
240 abolished in the Atg4a-C102S mutant background (Fig. 4f), as well as the climbing benefits
241 (Supplementary Fig. 4g). While catalase up-regulation led to decreased egg laying (Supplementary
242 Fig. 4h), this was observed in both the Atg4a-WT and C102S backgrounds, therefore any changes
243 in fecundity cannot explain the lifespan extension. Overall, redox-regulation of autophagy via
244 Atg4a-Cys102 mediates the longevity upon catalase over-expression. Enhancing autophagy is an
245 evolutionarily conserved intervention associated with health and survival benefits, and here we
246 demonstrate that selective redox-mediated up-regulation of autophagy can extend lifespan.

Discussion

Many attempts have been made to extend lifespan in model organisms by enhancing their antioxidant capacity, notably through the over-expression of antioxidant enzymes, including catalase[38-41]. These trials have been largely unsuccessful, casting doubt on the causative role of ROS and oxidative damage in ageing[42]. Therefore, our finding that catalase over-expression extends lifespan was at first surprising. The original study over-expressing catalase in *Drosophila* found no effect on lifespan and only modest resistance to oxidative stress by H_2O_2[38]. However, the study used an extra chromosomal copy under its endogenous promoter, resulting in lower over-expression of catalase (~1.75-fold at the mRNA level and ~1.5-fold increased enzyme activity). The degree of catalase over-expression is therefore likely to be important for the lifespan extension. Furthermore, the earlier study used only males, while our findings show a robust effect specifically in females. The results of these studies are therefore reconcilable.

The sex-specificity of lifespan benefits upon catalase up-regulation is striking. Indeed, we find that ubiquitous catalase over-expression does not extend lifespan or induce starvation sensitivity in males. A recent study showed that basal autophagy levels are significantly higher in male flies[43], shedding light on this sex-specificity of the catalase effect. This suggests that females have a broader 'metabolic plasticity', and are more likely to benefit from interventions that enhance autophagy.

Importantly, our study also challenges widespread assumptions regarding the directionality of antioxidant interventions. Indeed, we find that *in vivo* up-regulation of the antioxidant catalase, while directly conferring strong resistance to acute oxidative stress challenges as expected, also unexpectedly leads to an indirect oxidising shift in bulk cysteine redox state by interfering with homeostatic redox signalling. Consistent with our observations, a recent study in *C. elegans* has shown that excess dietary supplementation with *N*-acetyl cysteine (NAC) accelerates ageing by inhibiting *skn-1*-mediated transcription, the worm orthologue of Nrf2[44]. Therefore, caution is required in the interpretation of experiments involving the genetic or dietary manipulation of antioxidants.

Our unbiased redox proteomic analysis has revealed that the catalase flies undergo an oxidising shift in bulk cysteine redox state with age. Interestingly, this pattern is similar to our earlier observations in control flies under starvation[6]. Nutrient deprivation can directly affect redox homeostasis by depleting the provision of important building blocks for reducing equivalents, such as NADPH and glutathione, mediating an intracellular oxidising shift[45]. Therefore, we suggest that the catalase-induced thiol oxidising shift is perceived as an internal state of starvation, which triggers the induction of autophagy as a protective response (Fig. 4g). Autophagy plays a fundamental role in healthy physiology, such as cellular differentiation, tissue remodelling, and mitochondrial homeostasis, as well as in the response to stress and the clearance of cellular damage[27].

282 Consequently, enhanced autophagy is a common denominator of many evolutionary conserved
283 interventions that extend lifespan[26,27], both genetically, such as down-regulation of insulin
284 signalling[46], and pharmacologically, for instance rapamycin treatment[47]. Furthermore, direct up-
285 regulation of autophagy has been shown to exert health benefits and extend lifespan in a range of
286 model organisms including worms, flies and mice[34,48-50]. Several components of the autophagy
287 pathway are known to be redox-regulated, including Atg3 and Atg7[51], as well as the focus of our
288 study Atg4[35,52].

289 Overall, we have shown that shifting the *in vivo* redox state of *Drosophila* by over-expression
290 of catalase extends lifespan and healthspan in females through redox-regulation of autophagy via a
291 key redox-responsive cysteine in Atg4a. Our findings further emphasise the importance of fine-
292 tuning autophagy in health and disease, and demonstrate how manipulation of redox signalling *in*
293 *vivo* can ameliorate the effects of ageing. Furthermore, our data are consistent with a growing view
294 in the ageing field that many effects of ROS on longevity are likely to be through alterations in redox
295 signalling rather than through diminished oxidative damage[9,10,53].

296

297 # Methods

298 **Fly strains and husbandry**

299 The *white Dahomey* (w^{Dah}) strain of *Drosophila melanogaster* was used as the WT background. The
300 *Dahomey* stock was collected in 1970 in Dahomey (presently the Republic of Benin), and
301 maintained since then as large population cages, ensuring outbreeding and overlapping generations.
302 The w^{Dah} stock was derived by incorporation of the w^{1118} mutation into the outbred *Dahomey*
303 background by back-crossing. Flies were either negative (w^{Dah}) or positive (w^{Dah+}) for the bacterial
304 cytoplasmic endosymbiont *Wolbachia*, with infection status confirmed by PCR using published
305 primers against *wsp*[18]. The w^{Dah} stock was originally achieved by tetracycline treatment of the w^{Dah+}
306 stock[18]. The following transgenic lines were used: UAS-cat (BDSC 24621), UAS-catRNAi (VDRC
307 6283), gstD-GFP[37], UAS-Atg5RNAi[32], UAS-mito-cat[54], UAS-mito-QC[31]. The following driver
308 lines were used: da-GAL4[55], da-GS[56], act5c-GAL4 (BDSC 4414), Uro-GAL4[57], dilp2-GAL4[58],
309 elav-GS (BDSC 43642), $S_1$106-GS (BDSC 8151), TIGS-2[59], and MHC-GS[60]. All transgenic lines
310 were back-crossed into the appropriate w^{Dah} or w^{Dah+} background for at least 6-10 generations.
311 Experimental flies were incubated at 25ºC on a 12 h light:12 h dark cycle with 65% humidity.

312

313 **Generation of the Atg4a lines**

314 The Atg4a-C102S mutant fly line was generated by a fully transgenic CRISPR/Cas9 approach using
315 two guide RNAs (gRNAs)[61] targeting the Atg4a (CG4428) gene. The C102S mutation together with
316 an amino-terminal FLAG-tag were introduced using a donor construct for homology directed repair.

317 As a control, a fly line carrying only the FLAG-tag, referred to as Atg4a-WT, was generated using
318 the same approach. The gRNA construct was generated by PCR with Phusion polymerase (NEB)
319 and primers SOL897 and SOL898 (see Supplementary Table 4 for primer sequences) and the
320 plasmid pCDF4 as template[61]. The resulting PCR product was cloned into the pCDF4 vector using
321 the Gibson Assembly kit (NEB) and the resulting plasmid was then used to generate ATG4-gRNA
322 transgenic flies via injection into the *y*[1], *sc*[1], *v*[1], *P{y[+t7.7]=nos-phiC31\int.NLS}X;*
323 *P{y[+t7.7]=CaryP}attP2* fly line (BDSC 25710). Atg4a donor constructs were cloned in a two-step
324 approach. First, a 2792 bp part encompassing the Atg4a gene locus was amplified by PCR using
325 SOL926 and SOL927 on BAC clone CH321-39B1 (BACPAC Resources) as a template and cloned
326 into the pBluescript II KS vector via *NotI* and *KpnI* restriction mediated ligation. In the next step,
327 gene synthesis (Eurofins Genomics) was used to synthetise 806 bp long fragments encoding an
328 amino-terminal FLAG-tag, the C102S mutation and mutations within the PAM sites to introduce
329 the Atg4a-C102S mutation, or an amino-terminal FLAG-tag and mutations within the PAM sites to
330 generate the Atg4a-WT construct, respectively. These fragments were then used to replace the wild-
331 type sequence in the 2792 bp construct using the endogenous restriction sites *BstBI* and *MfeI*. In
332 order to introduce the mutation, Atg4a-gRNA transgenic flies were crossed with flies expressing
333 Cas9 under the ubiquitous actin promotor, and their progeny was injected with the Atg4a-C102S
334 and Atg4a-WT donor constructs. PCR screening with primers SOL955 and SOL929 that specifically
335 target the FLAG-tag sequence was used to identify positive CRISPR events and the presence of the
336 C102S mutation was confirmed by sequencing. All injections were performed by the transgenic fly
337 facility of the Max Planck Institute for Biology of Ageing.
338
339 **Fly media**
340 Flies were raised on standard sugar-yeast-agar medium (SYA) consisting of: 5% w/v sucrose
341 (granulated sugar, Silver Spoon), 10% w/v brewer's yeast (#903312, MP Biomedicals), 1.5% w/v
342 agar (A7002, Sigma), supplemented with nipagin (H5501, Sigma; 30 mL/L of 10% w/v nipagin in
343 95% EtOH) and propionic acid (P1386, Sigma; 0.3% v/v) as mould inhibitors, added once the food
344 had cooled down to ~60ºC[23]. Expression via the inducible GeneSwitch system was achieved by
345 addition of the drug RU (RU486/mifepristone; M8048, Sigma) to standard SYA once cooled down
346 to ~60ºC, typically at 200 µM from a 0.1 M stock in EtOH. For dietary restriction (DR) experiments,
347 the yeast content was varied to give 1% (0.1x), 5% (0.5x), 7.5% (0.75x), 10% (1x = SYA) or 15%
348 (1.5 SYA) w/v yeast[62].

349 **Experimental flies**

350 For all experiments, eggs were collected over a defined period (<24 h) to ensure a synchronous
351 population and reared at constant density in 200 mL bottles with SYA[62]. Eclosing adults of a defined
352 age were kept as a mixed population for ~48 h to allow mating, then separated into males and females
353 under mild CO_2 anaesthesia, and maintained as separate sexes from then onwards.

354

355 **Lifespan & stress assays**

356 Lifespan assays were set up as above, typically with n~10-15 flies per vial and a total of n~100-250
357 flies per condition. Flies were transferred to fresh food without gassing every ~2-3 days, with deaths
358 and censors recorded. Stress assays were performed on d7 flies (typically n>100 per condition in
359 groups of ~15-20 flies per vial), with deaths scored regularly following initiation of treatment. See
360 Supplementary Table 1 for full survival assay information. For H_2O_2 resistance, flies were
361 transferred onto medium containing 5% v/v H_2O_2 (H1009, Sigma), 5% w/v sucrose, 1.5% w/v agar.
362 For paraquat stress, flies were either transferred onto standard SYA food supplemented with 20 mM
363 paraquat (856177, Sigma), or injected with 75 nL of 1 mg/mL paraquat in Ringers buffer
364 (3 mM $CaCl_2$, 182 mM KCl, 46 mM NaCl, 10 mM Tris base, pH 7.2 HCl) and maintained on
365 standard SYA[63]. Starvation stress was assayed by transferring flies to 1.5% w/v agar medium, which
366 lacks nutrients but allows hydration. Chloroquine (C6628, Sigma) was prepared as 10 mM in SYA
367 or 5% w/v sugar, 1.5% w/v agar. Hyperoxia was performed by incubating flies on standard SYA
368 vials in a glove box chamber set at 90% O_2 using a ProOx controller (BioSpherix). The majority of
369 lifespans (Figs. 1a,b,e, 2a,b,h,i, 4e,f and Supplementary Figs. 1j-l) and stress assays (Figs. 1f,g, 2c,
370 4d and Supplementary Figs. 2f,h, 4d) were repeated at least twice as independent biological
371 experiments, except Figs. 1h,i and Supplementary Figs. 1e,f,h,i,n-s which were performed once.

372

373 **Development time**

374 Eggs were collected from flies in cages onto grape juice agar plates over a defined time window
375 (~4 h). After ~24 h, the resulting L1 larvae were picked onto SYA food at a density of 50 per vial
376 (n=500 total per genotype), and the time to adult eclosion was monitored.

377

378 **Climbing assay**

379 Climbing ability (negative geotaxis) was assayed essentially as described[63]. Briefly, groups of
380 15 flies were transferred to a sawn-open 25 mL serological pipette (35 cm long, 1.5 cm diameter),
381 with the base sealed by parafilm. The flies were tapped down within the column and observed during
382 45 s, after which their location was recorded. The column was separated into three sections: top
383 10 cm, middle, bottom 3 cm. Each cohort was evaluated 3 times, using 5 groups per genotype. The
384 climbing performance index was calculated as: $1/2\ (n^{total} + n^{top} - n^{bottom}/n^{total})$.

385 **Metabolic and molecular assays**

386 Flies for molecular experiments were rapidly transferred to pre-chilled microtubes via a small plastic
387 funnel and snap frozen in liquid nitrogen, then stored at –80°C until required. Flies were always
388 frozen at approximately the same time of day to minimise any circadian variation. For some assays,
389 frozen flies were separated into body segments using forceful manual impact[64].

390

391 **Quantitative PCR (QPCR)**

392 Total RNA was extracted using Trizol (Ambion) according to the manufacturer's instructions
393 (typically n=10 flies per sample, with n=4-5 replicates per condition). For some experiments, RNA
394 was extracted from head and thorax tissue (i.e. abdomens removed), to avoid interference from the
395 ovaries as the UAS/GAL4 system does not express in the germline. The concentration of total RNA
396 purified for each sample was measured spectrophotometrically. 3 µg of total RNA was then
397 subjected to DNA digestion using DNAse I (Ambion), immediately followed by reverse
398 transcription using the Superscript II system (Invitrogen) with oligo dT primers. QPCR was
399 performed using Fast SYBR Green Master Mix (Applied Biosystems) in a 7900HT Fast Real-Time
400 PCR machine, and results processed by SDS2.4 software (Applied Biosystems), or using SYBR
401 Green Supermix (1725124, Biorad) analysed with the QuantStudio 7 Flex Real-Time PCR System
402 (Thermo Scientific). The primers were designed using Primer BLAST[65] and are listed in
403 Supplementary Table 5.

404

405 **Western blotting**

406 Frozen fly samples were homogenised directly into 2X Laemmli loading buffer (Bio-Rad)
407 supplemented with 5% v/v β-mercaptoethanol (Sigma) using a pellet pestle and motor (usually 5/10
408 females into 100/200 µL) and separated by standard SDS-PAGE. The following primary antibodies
409 were used at the indicated dilutions: anti-actin (Ab1801, Ab8224, or Ab8227, AbCam; 1:1,000),
410 anti-Atg8 (a generous gift from K. Köhler[66]; 1:1,000), anti-catalase (C0979, Sigma; 1:10,000), anti-
411 GFP (#2955, Cell Signaling Technology; 1:1,000). The following secondary antibodies were used:
412 anti-mouse IgG (#7076, Cell Signaling Technology, or A4416, Sigma; 1:5,000), anti-rabbit IgG
413 (#7074, Cell Signaling Technology; 1:5,000). Blots were developed using standard ECL, followed
414 by analysis with FIJI software[67].

415

416 **Catalase activity**

417 Catalase activity was measured according to a published protocol[68], adapted for *Drosophila* samples.
418 Briefly, 5 whole flies were homogenised in 200 µL PBS supplemented with protease inhibitor
419 (HALT 1861284, ThermoScientific) using a TissueLyser (Precellys, 30sec), and centrifuged

420 (16,000 x g, 4ºC, 10 min). 50 µL supernatants (1:10 diluted in PBS for the da-GAL4>UAS-cat
421 genotype) were transferred to flow cytometry tubes (Falcon 5 mL polystyrene, round bottom, 12 x
422 75 mm), and combined with 50 µL 1% Triton-X100, followed by 50 µL 30% H_2O_2 solution (Sigma
423 H1009). After incubating at RT for 10 min, the height of the stable foam was marked, the tubes
424 photographed and analysed using FIJI. Enzyme activity was calculated by linear regression against
425 a standard curve of purified catalase (C40, Sigma) dissolved in PBS.
426
427 **Glutathione assay**
428 Total glutathione levels were measured as described[69], adapted for *Drosophila* samples. Briefly,
429 cohorts of 10 female flies (separated into head+thorax and abdomen fractions[64]) were homogenised
430 in 200 µL assay buffer (0.1 M potassium phosphate (pH 7.5), 5 mM EDTA), supplemented with
431 0.1% v/v Triton X-100 and 0.6% sulfosalicylic acid. Samples were centrifuged (16,000 x g, 4ºC,
432 10 min), and diluted 1:10 in assay buffer. 20 µL samples and glutathione standards (G6529, Sigma)
433 were transferred to a 96-well plate and overlayed with 120 µL of assay buffer containing DTNB
434 (D8130, Sigma; 2 mg/ 3mL) and 10 U glutathione reductase (G3664, Sigma; 10 U/3 mL), followed
435 by the addition of 60 µL NADPH (N7505, Sigma; 2 mg/3 mL assay buffer). The formation of TNB
436 was monitored kinetically at 412 nm over 5 min in a spectrophotometer (Fluostar Omega, BMG
437 Labtech). Glutathione levels were determined from the slope relative to the standard curve.
438
439 **Energy storage assays**
440 Whole body triacylglyceride (TAG) and glycogen levels were measured in d7 and d28 females (n=5
441 flies per sample, n=6-12 replicates per genotype) under control (fed) conditions and in response to
442 starvation. For the TAG assay, flies were homogenised in 0.05% v/v Tween-20 and assayed using
443 the Triglyceride Infinity Reagent (TR22421, ThermoScientific) in a 96-well plate measuring
444 absorbance at 540 nm. For the glycogen assay, d7 flies were homogenised in saturated sodium
445 sulphate, then the subsequent pellet was resuspended in anthrone reagent (319899, Sigma) and
446 assayed in a 96-well plate measuring absorbance at 620 nm[70].
447
448 **OxICAT sample preparation and LC-MS/MS analysis**
449 To measure the bulk redox state of protein cysteine residues, we performed unbiased redox
450 proteomics using OxICAT. Protein isolation, cysteine-residue labelling, peptide preparation and
451 LC-MS/MS analysis were performed exactly as described previously[6]. Briefly, cohorts of n=10
452 females flies were rapidly frozen in liquid N_2, and the frozen head and thorax tissue was separated
453 from the abdomens[64] to avoid signal from the ovaries. A total of n=5 biological replicates were
454 processed per condition. Samples were homogenised in ice-cold 100% w/v TCA to stabilise thiols

455 and solubilise proteins. Homogenates were centrifuged to pellet the chitin exoskeleton and other
456 insoluble components, and the resulting supernatant transferred to a fresh tube. Protein samples were
457 precipitated by decreasing the TCA concentration to 20% w/v with addition of H_2O, then washed
458 successively with 10% and 5% w/v TCA. This protein precipitation was shown to occur with
459 minimal protein losses or distortion of the protein complement[6].

460 Protein samples (~30-40 μg) were resuspended in denaturing alkylating buffer (DAB; 6 M
461 urea, 2% w/v SDS, 200 mM Tris-HCl, 10 mM EDTA, 100 μM DTPA, 10 μM neocuprine). Reduced
462 Cys residues were labelled with light ICAT reagent (4339036, AB Sciex) for 2 h at 37°C, 1400 rpm
463 in an Eppendorf Thermomixer. Proteins were precipitated and washed with ice-cold acetone,
464 solubilised in DAB with 1 mM TCEP (tris(2-carboxyethyl)phosphine) to reduce previously
465 reversibly oxidised Cys residues, which were then labelled with heavy ICAT reagent (4339036,
466 AB Sciex) as above, before again precipitating and washing in ice-cold acetone. ICAT-labelled
467 protein samples were resuspended in DAB and digested with trypsin overnight at 37°C. Digested
468 samples were enriched for Cys-containing peptides first on a cation exchange cartridge, and then
469 subsequently on an avidin affinity cartridge (both provided with the ICAT kit; 4339036, AB Sciex).
470 The eluted peptides were dried down overnight in a SpeedVac, and the biotin moiety of the ICAT
471 label cleaved.

472 Liquid chromatography-tandem mass spectrometry (LC-MS/MS) analysis of the OxICAT-
473 labelled peptides was performed exactly as published[6], using an Orbitrap LTQ XL (Thermo) after
474 chromatography on a nanoscale reverse-phase column. Raw files for each LC-MS/MS run were
475 analysed using MaxQuant software to determine the ratio of heavy over light OxICAT-labelled
476 peptides. Each biological sample (n=5 per condition) was run as 2 technical replicates, with the raw
477 files from both LC-MS/MS runs grouped into a combined dataset. Besides light or heavy ICAT
478 labelling of Cys residues, methionine oxidation was included as a possible modification, and up to
479 2 possible missed cleavages were allowed in the MaxQuant search parameters[6]. As a reference
480 sequence database, a FASTA file containing all protein sequences associated with *D. melanogaster*
481 was generated from UniProt, and used to identify peptides. In addition, the reference sequence
482 database was used to create an *in silico* tryptic digest of the *D. melanogaster* proteome, listing all
483 Cys-containing peptides (with 0, 1 or 2 missed cleavages), the Cys residue number, and the UniProt
484 protein ID[6]. Ratios of heavy over light ICAT-labelled peptides obtained from MaxQuant were
485 converted to % of the Cys residue reversibly oxidised (combining intensities from all peptide signals
486 containing the Cys residue of interest (e.g. miscleaved, methionine oxidation, different z values),
487 generating a mean % reversible oxidation for each unique Cys residue identified within the
488 biological replicates (Supplementary Table 2). Functional annotations were obtained from DAVID[71]
489 (https://david.ncifcrf.gov/tools.jsp; Supplementary Table 3).

490 **Confocal microscopy**

491 Autophagy and autophagic flux were assessed by LysoTracker Red and CytoID Green staining,
492 respectively[30]. Briefly, intact guts were dissected into 1x PBS (70011-036, Gibco) and stained in the
493 dark for 30 min with CytoID Green (ENZ-51036-K025, Enzo Life Sciences; 1:1,000 in 1x PBS),
494 followed by a second incubation for 3 min in PBS with LysoTracker Red (L7528, Invitrogen;
495 1:2,000 in 1x PBS) and HOECHST (H1399, Invitrogen; 1:1,000 from a 1 mg/mL stock in ultrapure
496 water) followed by three washes with PBS. Guts were mounted in mounting buffer (50% glycerol
497 in PBS) and immediately imaged. The number of LysoTracker punctae and HOECHST-stained
498 nuclei were quantified using using FIJI. As a positive control for CytoID staining, d7 female flies
499 were fed for 48 h on standard SYA medium supplemented with 30 mM choloroquine prior to gut
500 dissection and staining as described above. Quantification of punctae per cell was perfomed in FIJI.

501 Cellular ROS levels were assessed using CellROX Deep Red (C10422, Invitrogen; 1:500 in
502 PBS). Guts were dissected with minimal light exposure, and stained for 30 min at 25ºC in the dark,
503 then washed 3 times with 1x PBS prior to mounting (50% glycerol in PBS, with HOECHST 1:1,000
504 from a 1 mg/mL stock). Mean fluorescence intensity (MFI) was analysed using FIJI. As a positive
505 control, dissected guts were treated *ex vivo* with 10 μM H_2O_2 for 10 min in 1x PBS at RT prior to
506 CellRox staining as described above.

507 For catalase staining, whole guts were dissected in PBS and fixed in 4% paraformaldehyde
508 (30450002-2, 2B Scientific Ltd) for 20 min. After 3x 5 min washes with PBST (0.1% v/v Triton X-
509 100 in PBS), guts were blocked with 5% w/v BSA (A7906, Sigma) in PBST for 1 h. Guts were
510 incubated overnight at 4ºC with a primary anti-catalase antibody (C0979, Sigma; 1:250 in 5% w/v
511 BSA in PBS). After three washes with PBS, guts were incubated with an anti-mouse secondary
512 antibody (A10037, Invitrogen; Alexa568) for 1 h at RT, washed and mounted in VectaShield
513 containing DAPI (H1200-10, Vector Laboratories). Images were acquired on a Leica SP5 confocal
514 microscope (zoom: 20x optical plus 5x digital; resolution: 512 x 512 px at 700 Hz). Laser power
515 and optical settings were kept constant between images.

516

517 **Structural modelling**

518 The structure of *Drosophila* ATG4a was modelled using Phyre2[73] and visualised in Chimera X[74],
519 superimposed on the crystal structure of human ATG4A (PDB 2P82). Distances between the amino
520 acids belonging to the catalytic triad, as calculated in Chimera X[74], were comparable between human
521 and *Drosophila*:

522 Human: His281_NE2←→SG_Cys77 3.286 Å, His281_ND1←→OD1_Asp279 2.616 Å;

523 *Drosophila*: Hs273_NE2←→SG_Cys98 3.413 Å, His273_ND1←→OD1_Asp271 2.620 Å;

524

525 **MitoB injections**

526 To assay *in vivo* mitochondrial H_2O_2 levels, d7 females were injected with the ratiometric mass
527 spectrometry probe MitoB under mild CO_2 anaesthesia as described [36,64]. Flies were then returned
528 to standard food (cohorts of 10 flies, n=6-7 replicates per condition) and incubated for 4 h on SYA
529 medium at 25ºC, before snap freezing. A t=0 h control (n=3 replicates) was snap frozen immediately
530 to determine the background level of MitoP. Flies were homogenised, spiked with deuterated
531 internal standards, and extracted to quantify the MitoP/MitoB ratio[36,64].

532

533 **Statistical analysis**

534 Lifespan and stress assays were plotted as cumulative survival curves, and statistical analysis was
535 performed by Log-Rank test. Full details of survival data (n numbers, p values) are provided in
536 Supplementary Table 1. Other data were analysed by Student's *t*-test or ANOVA as appropriate in
537 GraphPad Prism v8-10.

538

539 Data availability

540 The proteomics dataset has been deposited to the ProteomeXchange Consortium[72] via the PRIDE
541 partner repository (accession number #PXD002195).

542

543 Acknowledgements

544 This project has received funding from the Medical Research Council UK (MC-A654-5QB90) to
545 HMC, and from the Max Planck Society to LP. MPM is supported by the Medical Research Council
546 UK (MC-U105663142) and by a Wellcome Trust Investigator Award (110159/Z/15/Z). FC was
547 supported by the Wellcome Trust/Royal Society (Sir Henry Dale Fellowship 102532/Z/12/Z and
548 102531/Z/13/A) and the DFG, German Research Foundation (EXC 2030 -390661388). We are
549 grateful to Pirrko Salmiheimo and Mumtaz Ahmad for help with preparation of fly media, Jigna
550 Patel for early technical support, Mike Harbour and Ian Fearnley for assistance with redox
551 proteomics, and Yu-Xuan Lu for advice on confocal imaging. We thank members of the Partridge
552 and Cochemé labs for valuable discussions throughout this project. We acknowledge the
553 Bloomington *Drosophila* Stock Center and the Vienna *Drosophila* Resource Center (VRDC) for fly
554 strains, and the BACPAC Resource Center for BAC clones. For the purpose of open access, the
555 author has applied a Creative Commons Attribution (CC BY) licence to any Author Accepted
556 Manuscript version arising.

557 ## Author contributions

558 Conceived the project: LP and HMC. Performed experiments and data analysis: CL, IB, JICQ,
559 LAGvL, AF, MB, JA, AM, HBK, PVS, AL, FC and HMC. Generated the CRISPR mutants: SG.
560 Conducted and analysed the redox proteomics: KEM and AMJ. Supervised the work: MPM, LP and
561 HMC. Wrote the manuscript: CL, MPM, LP and HMC, with input from all the authors.

562

563 ## Competing interests

564 The authors declare no competing interests.

565

566 ## References

567 1 Paulsen, C. E. & Carroll, K. S. Cysteine-mediated redox signaling: chemistry, biology, and
568 tools for discovery. *Chem. Rev.* **113**, 4633-4679 (2013). https://doi.org/10.1021/cr300163e

569 2 Holmstrom, K. M. & Finkel, T. Cellular mechanisms and physiological consequences of
570 redox-dependent signalling. *Nat. Rev. Mol. Cell Biol.* **15**, 411-421 (2014).
571 https://doi.org/10.1038/nrm3801

572 3 Sies, H. & Jones, D. P. Reactive oxygen species (ROS) as pleiotropic physiological
573 signalling agents. *Nat. Rev. Mol. Cell. Biol.* **21**, 363-383 (2020).
574 https://doi.org/10.1038/s41580-020-0230-3

575 4 Lennicke, C. & Cochemé, H. M. Redox metabolism: ROS as specific molecular regulators
576 of cell signaling and function. *Mol. Cell* **81**, 3691-3707 (2021).
577 https://doi.org/10.1016/j.molcel.2021.08.018

578 5 Brandes, N. *et al.* Time line of redox events in aging postmitotic cells. *eLife* **2**, e00306
579 (2013). https://doi.org/10.7554/eLife.00306

580 6 Menger, K. E. *et al.* Fasting, but Not Aging, Dramatically Alters the Redox Status of
581 Cysteine Residues on Proteins in *Drosophila melanogaster*. *Cell Rep.* **11**, 1856-1865
582 (2015). https://doi.org/10.1016/j.celrep.2015.05.033

583 7 Xiao, H. *et al.* A Quantitative Tissue-Specific Landscape of Protein Redox Regulation
584 during Aging. *Cell* **180**, 968-983 e924 (2020). https://doi.org/10.1016/j.cell.2020.02.012

585 8 Meng, J. *et al.* Global profiling of distinct cysteine redox forms reveals wide-ranging redox
586 regulation in *C. elegans*. *Nat. Commun.* **12**, 1415 (2021). https://doi.org/10.1038/s41467-
587 021-21686-3

588 9 Jones, D. P. Redox theory of aging. *Redox Biol.* **5**, 71-79 (2015).
589 https://doi.org/10.1016/j.redox.2015.03.004

590 10 Lennicke, C. & Cochemé, H. M. Redox signalling and ageing: insights from *Drosophila*.
591 *Biochem. Soc. Trans.* **48**, 367-377 (2020). https://doi.org/10.1042/BST20190052

592 11 Stocker, S., Van Laer, K., Mijuskovic, A. & Dick, T. P. The Conundrum of Hydrogen
593 Peroxide Signaling and the Emerging Role of Peroxiredoxins as Redox Relay Hubs.
594 *Antioxid. Redox Signal.* **28**, 558-573 (2018). https://doi.org/10.1089/ars.2017.7162

595 12 van Dam, L. *et al.* The Human 2-Cys Peroxiredoxins form Widespread, Cysteine-
596 Dependent- and Isoform-Specific Protein-Protein Interactions. *Antioxidants (Basel)* **10**
597 (2021). https://doi.org/10.3390/antiox10040627

598 13 Lennicke, C. & Cochemé, H. M. Redox regulation of the insulin signalling pathway. *Redox*
599 *Biol.* **42**, 101964 (2021). https://doi.org/10.1016/j.redox.2021.101964

600 14 Lopez-Otin, C., Blasco, M. A., Partridge, L., Serrano, M. & Kroemer, G. Hallmarks of
601 aging: An expanding universe. *Cell* **186**, 243-278 (2023).
602 https://doi.org/10.1016/j.cell.2022.11.001

603 15 Piper, M. D. W. & Partridge, L. *Drosophila* as a model for ageing. *Biochim. Biophys. Acta*
604 *Mol. Basis Dis.* **1864**, 2707-2717 (2018). https://doi.org/10.1016/j.bbadis.2017.09.016

605 16 Austad, S. N. & Fischer, K. E. Sex Differences in Lifespan. *Cell Metab.* **23**, 1022-1033
606 (2016). https://doi.org/10.1016/j.cmet.2016.05.019

607 17 Scialo, F. *et al.* Mitochondrial ROS Produced via Reverse Electron Transport Extend
608 Animal Lifespan. *Cell Metab.* **23**, 725-734 (2016).
609 https://doi.org/10.1016/j.cmet.2016.03.009

610 18 Toivonen, J. M. *et al.* No influence of Indy on lifespan in *Drosophila* after correction for
611 genetic and cytoplasmic background effects. *PLOS Genet.* **3**, e95 (2007).
612 https://doi.org/10.1371/journal.pgen.0030095

613 19 Ikeya, T., Broughton, S., Alic, N., Grandison, R. & Partridge, L. The endosymbiont
614 Wolbachia increases insulin/IGF-like signalling in *Drosophila*. *Proc. Biol. Sci.* **276**, 3799-
615 3807 (2009). https://doi.org/10.1098/rspb.2009.0778

616 20 Lopez-Otin, C., Blasco, M. A., Partridge, L., Serrano, M. & Kroemer, G. The hallmarks of
617 aging. *Cell* **153**, 1194-1217 (2013). https://doi.org/10.1016/j.cell.2013.05.039

618 21 Mair, W., Goymer, P., Pletcher, S. D. & Partridge, L. Demography of dietary restriction
619 and death in *Drosophila*. *Science* **301**, 1731-1733 (2003).
620 https://doi.org/10.1126/science.1086016

621 22 Fontana, L. & Partridge, L. Promoting health and longevity through diet: from model
622 organisms to humans. *Cell* **161**, 106-118 (2015). https://doi.org/10.1016/j.cell.2015.02.020

623 23 Grandison, R. C., Wong, R., Bass, T. M., Partridge, L. & Piper, M. D. Effect of a
624 standardised dietary restriction protocol on multiple laboratory strains of *Drosophila*
625 *melanogaster*. *PLOS One* **4**, e4067 (2009). https://doi.org/10.1371/journal.pone.0004067

626 24 Vilchez, D., Saez, I. & Dillin, A. The role of protein clearance mechanisms in organismal
627 ageing and age-related diseases. *Nat. Commun.* **5**, 5659 (2014).
628 https://doi.org/10.1038/ncomms6659

629 25 Kaushik, S. & Cuervo, A. M. Proteostasis and aging. *Nat. Med.* **21**, 1406-1415 (2015).
630 https://doi.org/10.1038/nm.4001

631 26 Madeo, F., Zimmermann, A., Maiuri, M. C. & Kroemer, G. Essential role for autophagy in
632 life span extension. *J. Clin. Invest.* **125**, 85-93 (2015). https://doi.org/10.1172/JCI73946

633 27 Hansen, M., Rubinsztein, D. C. & Walker, D. W. Autophagy as a promoter of longevity:
634 insights from model organisms. *Nat. Rev. Mol. Cell Biol.* **19**, 579-593 (2018).
635 https://doi.org/10.1038/s41580-018-0033-y

636 28 Aman, Y. *et al.* Autophagy in healthy aging and disease. *Nat Aging* **1**, 634-650 (2021).
637 https://doi.org/10.1038/s43587-021-00098-4

638 29 Scherz-Shouval, R. & Elazar, Z. Regulation of autophagy by ROS: physiology and
639 pathology. *Trends Biochem. Sci.* **36**, 30-38 (2011).
640 https://doi.org/10.1016/j.tibs.2010.07.007

641 30 Lu, Y. X. *et al.* A TORC1-histone axis regulates chromatin organisation and non-canonical
642 induction of autophagy to ameliorate ageing. *eLife* **10** (2021).
643 https://doi.org/10.7554/eLife.62233

644 31 Lee, J. J. *et al.* Basal mitophagy is widespread in *Drosophila* but minimally affected by
645 loss of Pink1 or parkin. *J. Cell Biol.* **217**, 1613-1622 (2018).
646 https://doi.org/10.1083/jcb.201801044

647 32 Scott, R. C., Schuldiner, O. & Neufeld, T. P. Role and regulation of starvation-induced
648 autophagy in the *Drosophila* fat body. *Dev. Cell* **7**, 167-178 (2004).
649 https://doi.org/10.1016/j.devcel.2004.07.009

650 33 Kang, C., You, Y. J. & Avery, L. Dual roles of autophagy in the survival of
651 *Caenorhabditis elegans* during starvation. *Genes & development* **21**, 2161-2171 (2007).
652 https://doi.org/10.1101/gad.1573107

653 34 Bjedov, I. *et al.* Fine-tuning autophagy maximises lifespan and is associated with changes
654 in mitochondrial gene expression in Drosophila. *PLOS Genet.* **16**, e1009083 (2020).
655 https://doi.org/10.1371/journal.pgen.1009083

656 35 Scherz-Shouval, R. *et al.* Reactive oxygen species are essential for autophagy and
657 specifically regulate the activity of Atg4. *EMBO J.* **26**, 1749-1760 (2007).
658 https://doi.org/10.1038/sj.emboj.7601623

659 36 Cochemé, H. M. *et al.* Measurement of H_2O_2 within living *Drosophila* during aging using a
660 ratiometric mass spectrometry probe targeted to the mitochondrial matrix. *Cell Metab.* **13**,
661 340-350 (2011). https://doi.org/10.1016/j.cmet.2011.02.003

662 37 Sykiotis, G. P. & Bohmann, D. Keap1/Nrf2 signaling regulates oxidative stress tolerance
663 and lifespan in *Drosophila*. *Dev. Cell* **14**, 76-85 (2008).
664 https://doi.org/10.1016/j.devcel.2007.12.002

665 38 Orr, W. C. & Sohal, R. S. The effects of catalase gene overexpression on life span and
666 resistance to oxidative stress in transgenic *Drosophila melanogaster*. *Arch. Biochem.*
667 *Biophys.* **297**, 35-41 (1992). https://doi.org/10.1016/0003-9861(92)90637-c

668 39 Orr, W. C., Mockett, R. J., Benes, J. J. & Sohal, R. S. Effects of overexpression of copper-
669 zinc and manganese superoxide dismutases, catalase, and thioredoxin reductase genes on
670 longevity in *Drosophila melanogaster*. *J. Biol. Chem.* **278**, 26418-26422 (2003).
671 https://doi.org/10.1074/jbc.M303095200

672 40 Doonan, R. *et al.* Against the oxidative damage theory of aging: superoxide dismutases
673 protect against oxidative stress but have little or no effect on life span in *Caenorhabditis*
674 *elegans*. *Genes & development* **22**, 3236-3241 (2008). https://doi.org/10.1101/gad.504808

675 41 Perez, V. I. *et al.* The overexpression of major antioxidant enzymes does not extend the
676 lifespan of mice. *Aging Cell* **8**, 73-75 (2009). https://doi.org/10.1111/j.1474-
677 9726.2008.00449.x

678 42 Gems, D. & Doonan, R. Antioxidant defense and aging in *C. elegans*: is the oxidative
679 damage theory of aging wrong? *Cell Cycle* **8**, 1681-1687 (2009).
680 https://doi.org/10.4161/cc.8.11.8595

681 43 Regan, J. C. *et al.* Sexual identity of enterocytes regulates autophagy to determine
682 intestinal health, lifespan and responses to rapamycin. *Nat Aging* **2**, 1145-1158 (2022).
683 https://doi.org/10.1038/s43587-022-00308-7

684 44 Gusarov, I. *et al.* Dietary thiols accelerate aging of C. elegans. *Nat. Commun.* **12**, 4336
685 (2021). https://doi.org/10.1038/s41467-021-24634-3

686 45 Filomeni, G., De Zio, D. & Cecconi, F. Oxidative stress and autophagy: the clash between
687 damage and metabolic needs. *Cell Death Differ.* **22**, 377-388 (2015).
688 https://doi.org/10.1038/cdd.2014.150

689 46 Toth, M. L. *et al.* Longevity pathways converge on autophagy genes to regulate life span in
690 *Caenorhabditis elegans*. *Autophagy* **4**, 330-338 (2008). https://doi.org/10.4161/auto.5618

691 47 Bjedov, I. *et al.* Mechanisms of life span extension by rapamycin in the fruit fly
692 *Drosophila melanogaster*. *Cell Metab.* **11**, 35-46 (2010).
693 https://doi.org/10.1016/j.cmet.2009.11.010

694 48 Simonsen, A. *et al.* Promoting basal levels of autophagy in the nervous system enhances
695 longevity and oxidant resistance in adult *Drosophila*. *Autophagy* **4**, 176-184 (2008).
696 https://doi.org/10.4161/auto.5269

697 49 Lapierre, L. R. *et al.* The TFEB orthologue HLH-30 regulates autophagy and modulates
698 longevity in *Caenorhabditis elegans*. *Nat. Commun.* **4**, 2267 (2013).
699 https://doi.org/10.1038/ncomms3267

700 50 Pyo, J. O. *et al.* Overexpression of Atg5 in mice activates autophagy and extends lifespan.
701 *Nat. Commun.* **4**, 2300 (2013). https://doi.org/10.1038/ncomms3300

702 51 Frudd, K., Burgoyne, T. & Burgoyne, J. R. Oxidation of Atg3 and Atg7 mediates
703 inhibition of autophagy. *Nat. Commun.* **9**, 95 (2018). https://doi.org/10.1038/s41467-017-
704 02352-z

705 52 Ligeon, L. A. *et al.* Oxidation inhibits autophagy protein deconjugation from phagosomes
706 to sustain MHC class II restricted antigen presentation. *Nat. Commun.* **12**, 1508 (2021).
707 https://doi.org/10.1038/s41467-021-21829-6

708 53 Orr, W. C., Radyuk, S. N. & Sohal, R. S. Involvement of redox state in the aging of
709 *Drosophila melanogaster*. *Antioxid. Redox Signal.* **19**, 788-803 (2013).
710 https://doi.org/10.1089/ars.2012.5002

711 54 Radyuk, S. N. *et al.* Mitochondrial peroxiredoxins are critical for the maintenance of redox
712 state and the survival of adult Drosophila. *Free Radic. Biol. Med.* **49**, 1892-1902 (2010).
713 https://doi.org/10.1016/j.freeradbiomed.2010.09.014

714 55 Wodarz, A., Hinz, U., Engelbert, M. & Knust, E. Expression of crumbs confers apical
715 character on plasma membrane domains of ectodermal epithelia of *Drosophila*. *Cell* **82**,
716 67-76 (1995). https://doi.org/10.1016/0092-8674(95)90053-5

717 56 Tricoire, H. *et al.* The steroid hormone receptor EcR finely modulates *Drosophila* lifespan
718 during adulthood in a sex-specific manner. *Mech. Ageing Dev.* **130**, 547-552 (2009).
719 https://doi.org/10.1016/j.mad.2009.05.004

720 57 Terhzaz, S. *et al.* Cell-specific inositol 1,4,5 trisphosphate 3-kinase mediates epithelial cell
721 apoptosis in response to oxidative stress in *Drosophila*. *Cell Signal.* **22**, 737-748 (2010).
722 https://doi.org/10.1016/j.cellsig.2009.12.009

723 58 Ikeya, T., Galic, M., Belawat, P., Nairz, K. & Hafen, E. Nutrient-dependent expression of
724 insulin-like peptides from neuroendocrine cells in the CNS contributes to growth
725 regulation in *Drosophila*. *Curr. Biol.* **12**, 1293-1300 (2002). https://doi.org/10.1016/S0960-
726 9822(02)01043-6

727 59 Poirier, L., Shane, A., Zheng, J. & Seroude, L. Characterization of the *Drosophila* gene-
728 switch system in aging studies: a cautionary tale. *Aging Cell* **7**, 758-770 (2008).
729 https://doi.org/10.1111/j.1474-9726.2008.00421.x

730 60 Osterwalder, T., Yoon, K. S., White, B. H. & Keshishian, H. A conditional tissue-specific
731 transgene expression system using inducible GAL4. *Proc. Natl. Acad. Sci. U. S. A.* **98**,
732 12596-12601 (2001). https://doi.org/10.1073/pnas.221303298

733 61 Port, F., Chen, H. M., Lee, T. & Bullock, S. L. Optimized CRISPR/Cas tools for efficient
734 germline and somatic genome engineering in *Drosophila*. *Proc. Natl. Acad. Sci. U. S. A.*
735 **111**, E2967-2976 (2014). https://doi.org/10.1073/pnas.1405500111

736 62 Bass, T. M. *et al.* Optimization of dietary restriction protocols in *Drosophila*. *J. Gerontol.*
737 *A Biol. Sci. Med. Sci.* **62**, 1071-1081 (2007). https://doi.org/10.1093/gerona/62.10.1071

738 63 Kerr, F. *et al.* Direct Keap1-Nrf2 disruption as a potential therapeutic target for
739 Alzheimer's disease. *PLOS Genet.* **13**, e1006593 (2017).
740 https://doi.org/10.1371/journal.pgen.1006593

741 64 Cochemé, H. M. *et al.* Using the mitochondria-targeted ratiometric mass spectrometry
742 probe MitoB to measure H_2O_2 in living *Drosophila*. *Nat. Protoc.* **7**, 946-958 (2012).
743 https://doi.org/10.1038/nprot.2012.035

744 65 Ye, J. *et al.* Primer-BLAST: a tool to design target-specific primers for polymerase chain
745 reaction. *BMC Bioinform.* **13**, 134 (2012). https://doi.org/10.1186/1471-2105-13-134

746 66 Barth, J. M., Szabad, J., Hafen, E. & Kohler, K. Autophagy in *Drosophila* ovaries is
747 induced by starvation and is required for oogenesis. *Cell Death Differ.* **18**, 915-924 (2011).
748 https://doi.org/10.1038/cdd.2010.157

749 67 Schindelin, J. *et al.* Fiji: an open-source platform for biological-image analysis. *Nat.*
750 *Methods* **9**, 676-682 (2012). https://doi.org/10.1038/nmeth.2019

751 68 Iwase, T. *et al.* A simple assay for measuring catalase activity: a visual approach. *Sci. Rep.*
752 **3**, 3081 (2013). https://doi.org/10.1038/srep03081

753 69 Rahman, I., Kode, A. & Biswas, S. K. Assay for quantitative determination of glutathione
754 and glutathione disulfide levels using enzymatic recycling method. *Nat. Protoc.* **1**, 3159-
755 3165 (2006). https://doi.org/10.1038/nprot.2006.378

756 70 Castillo-Quan, J. I. *et al.* Lithium Promotes Longevity through GSK3/NRF2-Dependent
757 Hormesis. *Cell Rep.* **15**, 638-650 (2016). https://doi.org/10.1016/j.celrep.2016.03.041

758 71 Sherman, B. T. *et al.* DAVID: a web server for functional enrichment analysis and
759 functional annotation of gene lists (2021 update). *Nucleic Acids Res.* **50**, W216-W221
760 (2022). https://doi.org/10.1093/nar/gkac194

761 72 Vizcaino, J. A. *et al.* ProteomeXchange provides globally coordinated proteomics data
762 submission and dissemination. *Nat. Biotechnol.* **32**, 223-226 (2014).
763 https://doi.org/10.1038/nbt.2839

764 73 Kelley, L. A., Mezulis, S., Yates, C. M., Wass, M. N. & Sternberg, M. J. The Phyre2 web
765 portal for protein modeling, prediction and analysis. *Nat. Protoc.* **10**, 845-858 (2015).
766 https://doi.org/10.1038/nprot.2015.053

767 74 Pettersen, E. F. *et al.* UCSF ChimeraX: Structure visualization for researchers, educators,
768 and developers. *Protein Sci.* **30**, 70-82 (2021). https://doi.org/10.1002/pro.3943

Figure 1

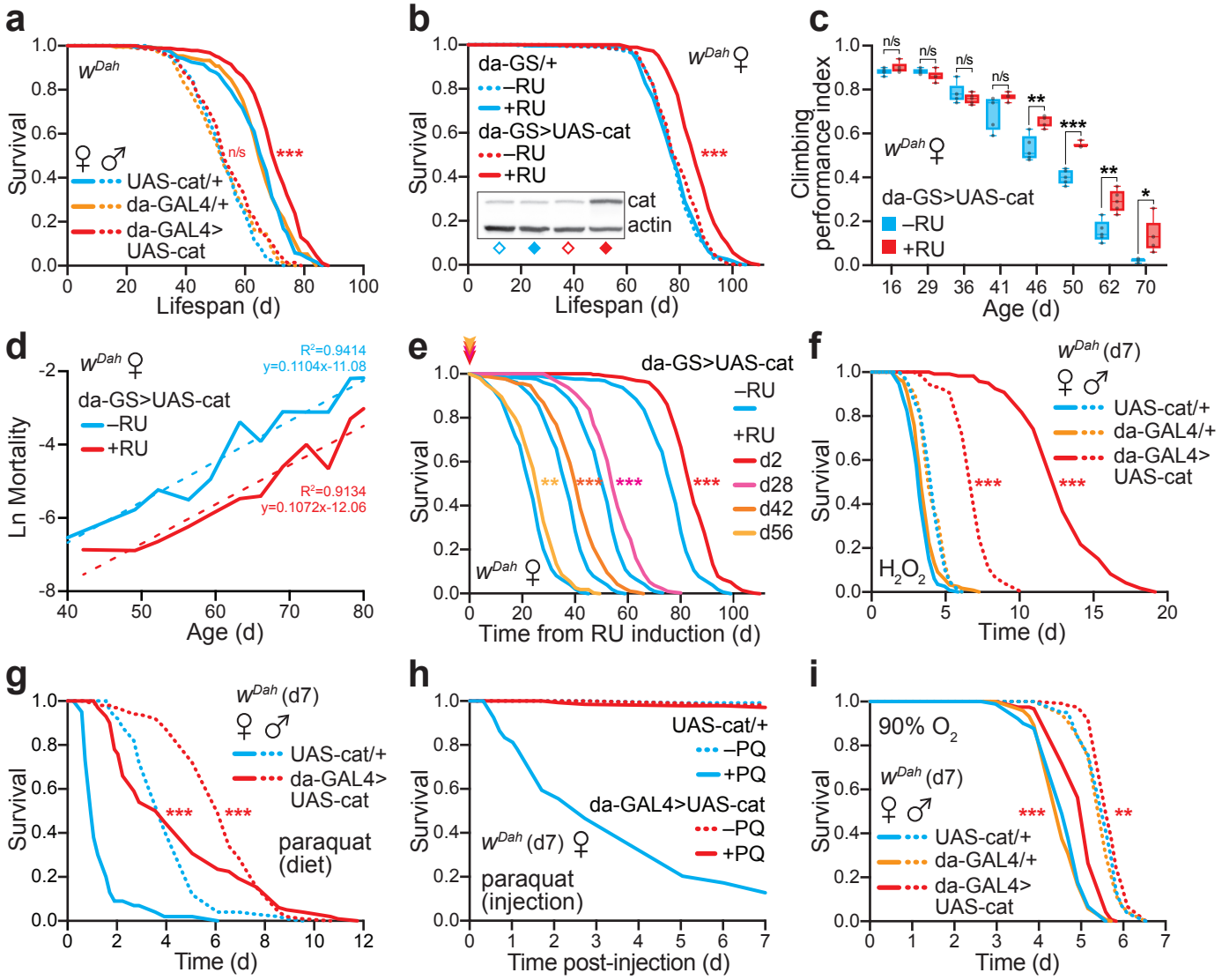
a
Survival
Lifespan (d)
wDah
♀ ♂
UAS-cat/+
da-GAL4/+
da-GAL4>
UAS-cat
n/s
***
b
Survival
Lifespan (d)
da-GS/+
–RU
+RU
da-GS>UAS-cat
–RU
+RU
wDah ♀
cat
actin
***
c
Climbing performance index
Age (d)
n/s
**
***
*
wDah ♀
da-GS>UAS-cat
–RU
+RU
d
Ln Mortality
Age (d)
wDah ♀
da-GS>UAS-cat
–RU
+RU
R²=0.9414
y=0.1104x-11.08
R²=0.9134
y=0.1072x-12.06
e
Survival
Time from RU induction (d)
da-GS>UAS-cat
–RU
+RU
d2
d28
d42
d56
wDah ♀
**
***
f
Survival
Time (d)
wDah (d7)
♀ ♂
UAS-cat/+
da-GAL4/+
da-GAL4>
UAS-cat
H2O2
***
g
Survival
Time (d)
wDah (d7)
♀ ♂
UAS-cat/+
da-GAL4>
UAS-cat
paraquat
(diet)
***
h
Survival
Time post-injection (d)
UAS-cat/+
–PQ
+PQ
da-GAL4>UAS-cat
–PQ
+PQ
wDah (d7) ♀
paraquat
(injection)
i
Survival
Time (d)
90% O2
wDah (d7)
♀ ♂
UAS-cat/+
da-GAL4/+
da-GAL4>
UAS-cat
***
**

769 **Fig. 1 | Ubiquitous catalase up-regulation extends lifespan in flies, independently of oxidative**
770 **stress resistance. a,** Constitutive, ubiquitous catalase over-expression (da-GAL4>UAS-cat)
771 extended the survival of female flies in a w^{Dah} (*white Dahomey*) WT background relative to the
772 UAS-cat/+ ($p=5.7x10^{-7}$) and da-GAL4/+ ($p=3.3x10^{-6}$) controls. The control lines were not
773 significantly different from each other (p=0.7504). No effect was observed in males (p>0.05 for all
774 comparisons). Lifespans were performed with n=200 flies per condition. **b,** Inducible catalase over-
775 expression from early adulthood (d2) using the GeneSwitch system extended the lifespan of female
776 flies (da-GS>UAS-cat ±RU, $p=1.1x10^{-16}$). RU had no effect on the da-GS/+ control line (p=0.7161).
777 Lifespans were performed with n=225-300 flies per condition. Inset: catalase over-expression
778 assessed by Western blotting in whole d9 females (=d7 of RU induction), with actin as a loading
779 control. **c,** Healthspan, inferred from climbing performance, was improved in catalase over-
780 expressing females. Climbing was assayed on da-GS>UAS-cat females ±RU to control for effects
781 of eye colour on this behaviour. Data are presented as box-and-whisker plots (min/max error bars)
782 of n=5 replicates per condition, each with n=15 flies per sample, analysed by unpaired Student's *t*-
783 test. **d,** Mortality trajectories of the da-GS>UAS-cat ±RU survival curves from (**b**), fitted with a
784 linear regression trendline (dotted line). **e,** Late onset over-expression of catalase using the inducible
785 GeneSwitch system from either middle-age (d28 and d42) and old-age (d56) extended the lifespan
786 of female flies ($p=7.2x10^{-8}$, $p=1.0x10^{-7}$ and $p=1.4x10^{-3}$, respectively against the –RU control).
787 Lifespans were performed with n=270 flies per condition, and were plotted from point of RU
788 induction relative to the remaining –RU control flies at that age (see Supplementary Fig. 1l for the
789 full survival data). **f,** Catalase over-expressing flies were strongly resistant to exogenous H_2O_2 stress
790 relative to controls (da-GAL4>UAS-cat *v.* UAS-cat/+; $p=5.0x10^{-61}$ females, $p=3.2x10^{-33}$ males).
791 H_2O_2 treatment (5% v/v in sucrose/agar medium) was initiated at d7, with n=105 males (n=75 for
792 da-GS>UAS-cat) and n=120 females per condition. **g,** Catalase over-expressing flies were resistant
793 to chronic dietary paraquat stress relative to control flies (da-GAL4>UAS-cat *v.* UAS-cat/+;
794 $p=6.93x10^{-31}$ females, $p=7.99x10^{-16}$ males). Paraquat treatment (20 mM in SYA food) was initiated
795 at d7, with n=100 flies per condition. **h,** Catalase over-expressing flies (da-GAL4>UAS-cat) were
796 resistant to acute paraquat stress relative to controls (UAS-cat/+). d7 females were injected with
797 75 nL of 1 mg/mL paraquat in Ringers buffer (+PQ, n=150 flies) or mock injected with buffer alone
798 (–PQ, n=120 flies). **i,** Catalase over-expressing flies were resistant to environmental hyperoxia stress
799 relative to controls (da-GAL4>UAS-cat *v.* UAS-cat/+; $p=1.7x10^{-8}$ females, $p=8.1x10^{-3}$ males).
800 Incubation at 90% O_2 was initiated at d7, with n=120 flies per condition (except n=90 for UAS-cat/+
801 females). All survival assays (**a**,**b**,**e**,**f**,**g**,**i**) were analysed by Log-Rank test (see Supplementary
802 Table 1 for full n numbers and p values). n/s, p>0.05; *, p<0.05; **, p<0.01; ***, p<0.001.

Figure 2

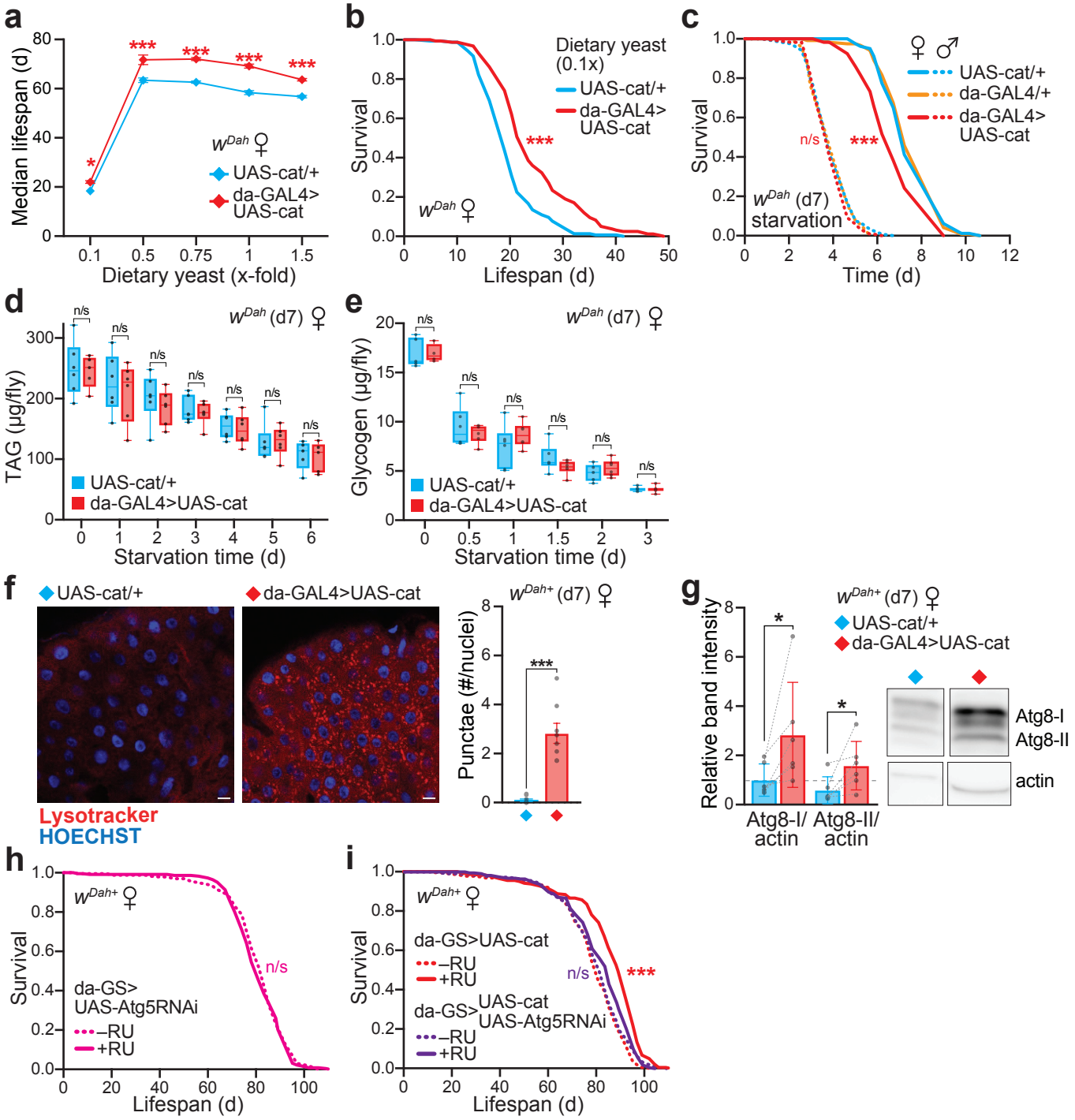
a
Median lifespan (d)
Dietary yeast (x-fold)
wDah ♀
UAS-cat/+
da-GAL4> UAS-cat
b
Survival
Lifespan (d)
Dietary yeast (0.1x)
UAS-cat/+
da-GAL4> UAS-cat
wDah ♀
c
Survival
Time (d)
♀ ♂
UAS-cat/+
da-GAL4/+
da-GAL4> UAS-cat
wDah (d7) starvation
n/s
d
TAG (µg/fly)
Starvation time (d)
wDah (d7) ♀
UAS-cat/+
da-GAL4>UAS-cat
e
Glycogen (µg/fly)
Starvation time (d)
wDah (d7) ♀
UAS-cat/+
da-GAL4>UAS-cat
f
UAS-cat/+
da-GAL4>UAS-cat
Lysotracker
HOECHST
wDah+ (d7) ♀
Punctae (#/nuclei)
g
Relative band intensity
wDah+ (d7) ♀
UAS-cat/+
da-GAL4>UAS-cat
Atg8-I/ actin
Atg8-II/ actin
Atg8-I
Atg8-II
actin
h
Survival
Lifespan (d)
wDah+ ♀
da-GS> UAS-Atg5RNAi
–RU
+RU
n/s
i
Survival
Lifespan (d)
wDah+ ♀
da-GS>UAS-cat
–RU
+RU
da-GS> UAS-cat UAS-Atg5RNAi
–RU
+RU
n/s

803 **Fig. 2 | Catalase lifespan extension requires autophagy. a,** Catalase over-expressor (da-
804 GAL4>UAS-cat) and control (UAS-cat/+) females displayed a normal response to dietary restriction
805 (DR). Median lifespan is plotted against the yeast content of the diet, with 1x corresponding to
806 standard SYA food. Data are the means ±range of 2 independent lifespan experiments, each set up
807 with n=150-160 flies per genotype, analysed by two-way ANOVA (Fisher's LSD). **b,** Survival curve
808 on 0.1x-fold yeast from (**a**). The catalase over-expressor females (da-GAL4>UAS-cat) were longer-
809 lived than controls (UAS-cat/+) under low yeast nutritional conditions ($p=3.6x10^{-10}$, n=160 flies per
810 genotype). **c,** Catalase over-expressor females (da-GAL4>UAS-cat) were sensitive to starvation
811 stress relative to UAS-cat/+ and da-GAL4/+ controls ($p=5.6x10^{-5}$ and $p=7.6x10^{-7}$, respectively). No
812 difference was observed in males (p>0.05 for all comparisons). Assays were performed at d7 with
813 n=120 flies per condition (except n=80 for UAS-cat/+ females). **d-e,** Triacylglyceride (TAG, **d**) and
814 glycogen (**e**) levels in whole females assayed at d7 (t=0) and depletion in response to starvation
815 treatment. Data are presented as box-and-whisker plots (min/max error bars) of n=4-6 replicates per
816 genotype, each with n=5 females per sample, analysed by unpaired Student's *t*-test (p>0.05). **f-g,**
817 Catalase over-expressor females (da-GAL4>UAS-cat) displayed enhanced autophagy induction
818 compared to UAS-cat/+ controls at d7. **f**, LysoTracker Red staining of midguts quantified as the
819 number of punctae relative to HOECHST-stained nuclei (scale bar = 10 μm). Data are means ±SD
820 of n=8 biological replicates, analysed by unpaired Student's *t*-test (***, p<0.001). **g**, Western
821 blotting against Atg8, normalised to actin. Data are means ±SD of n=6 biological replicates, each
822 with n=10 abdomens per sample, analysed by paired Student's *t*-test (*, p<0.05). Right, typical
823 bands probed against Atg8 with actin as a loading control (see Supplementary Fig. 4e for the full
824 blot). **h,** Global Atg5 knock-down did not decrease lifespan in a WT background under control
825 conditions (da-GS>UAS-Atg5RNAi ±RU; p=0.4177). Lifespan assays were performed on n=225-
826 240 females. **i,** Lifespan extension upon catalase over-expression (da-GS>UAS-cat ±RU; $p=7.2x10^{-}$
827 ^{15}) was abolished in an autophagy-deficient background (da-GS>UAS-cat+UAS-Atg5RNAi ±RU;
828 p=0.1701). Survival assays (**b**,**c**,**h**,**i**) were analysed by Log-Rank test (see Supplementary Table 1
829 for full n numbers and p values). n/s, p>0.05; ***, p<0.001.

Figure 3

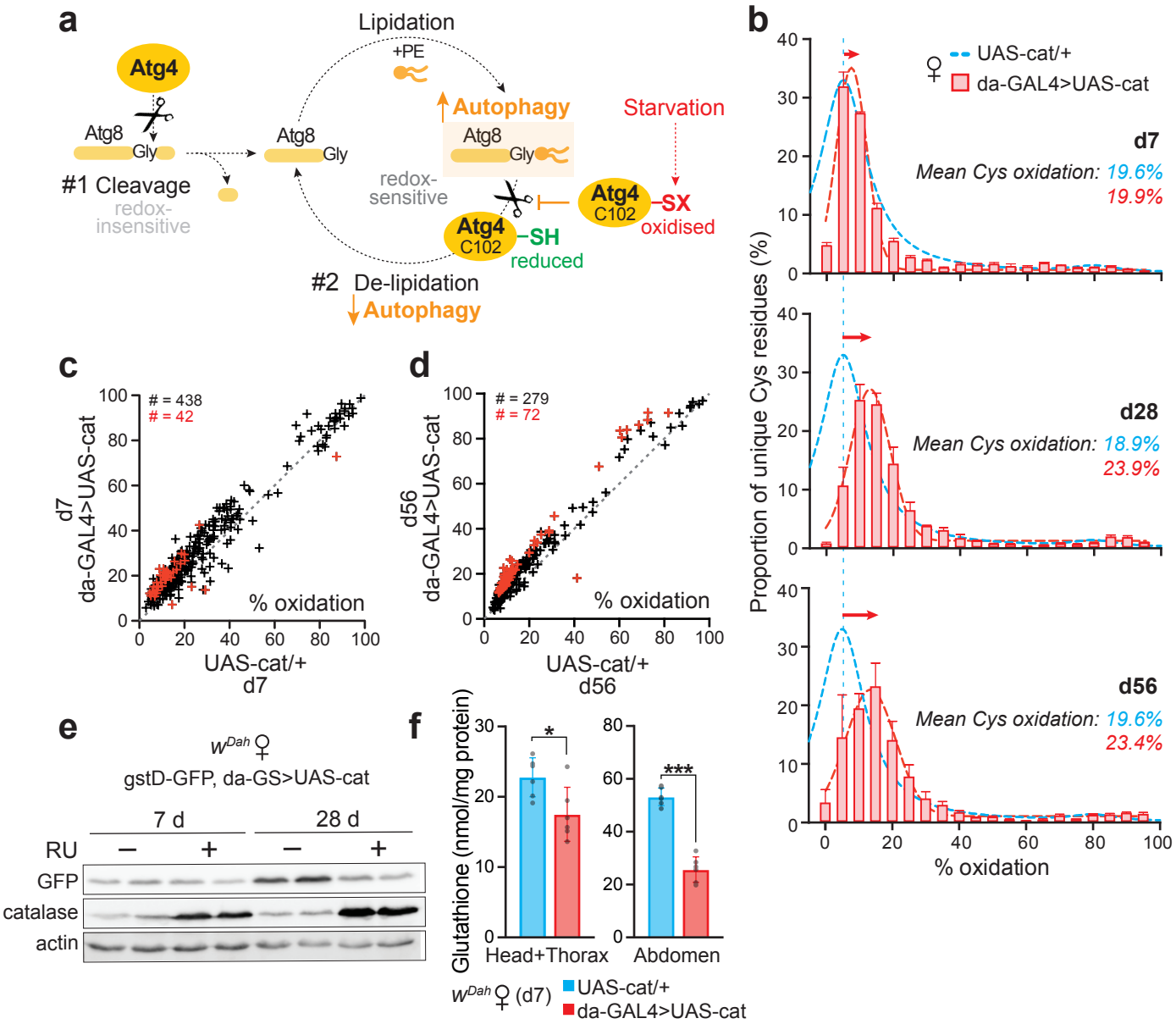
a
Lipidation
+PE
Atg4
Atg8
Gly
#1 Cleavage
redox-insensitive
Autophagy
Starvation
redox-sensitive
Atg4 C102
–SX
oxidised
–SH
reduced
#2 De-lipidation
Autophagy
b
UAS-cat/+
da-GAL4>UAS-cat
d7
Mean Cys oxidation: 19.6%
19.9%
d28
Mean Cys oxidation: 18.9%
23.9%
d56
Mean Cys oxidation: 19.6%
23.4%
Proportion of unique Cys residues (%)
% oxidation
c
= 438
= 42
d7 da-GAL4>UAS-cat
UAS-cat/+ d7
% oxidation
d
= 279
= 72
d56 da-GAL4>UAS-cat
UAS-cat/+ d56
% oxidation
e
wDah ♀
gstD-GFP, da-GS>UAS-cat
7 d
28 d
RU
–
+
–
+
GFP
catalase
actin
f
Glutathione (nmol/mg protein)
Head+Thorax
Abdomen
wDah ♀ (d7)
UAS-cat/+
da-GAL4>UAS-cat

830 **Fig. 3 | Catalase flies undergo an oxidising shift in global thiol redox state. a,** Scheme showing
831 the dual function of Atg4 in autophagy: 1) initial redox-independent cleavage of Atg8, to expose a
832 C-terminal glycine residue enabling lipidation by PE (phosphatidyl-ethanolamine) via the E1-like
833 enzyme Atg7 and the E2-like enzyme Atg3. The conjugated Atg8-PE is involved in autophagosome
834 elongation/closure; 2) redox-dependent de-lipidation of Atg8-PE, allowing interaction and fusion of
835 the autophagosome with the endosomal-lysosomal compartments, and recycling of cleaved Atg8.
836 Oxidation of a redox-regulatory cysteine (C102 in *Drosophila* Atg4a) selectively inactivates the
837 Atg8-PE de-conjugation activity of Atg4, promoting autophagosome biogenesis and therefore
838 enhancing Atg4-mediated autophagy. **b,** Redox proteomic (OxICAT) analysis of d7, d28 and d56
839 catalase over-expressing females (da-GAL4>UAS-cat) compared to control (UAS-cat/+).
840 Distribution of total cysteine residue oxidation levels, plotted as the proportion of the total number
841 of peptides containing unique cysteine residues in each 5% quantile of percentage oxidation. Data
842 are means ±SEM of n=5 biological replicates. **c-d,** Oxidation state of cysteine residues present,
843 comparing control versus catalase over-expressor females at d7 (**c**) and d56 (**d**). Data points above
844 the diagonal dotted line (slope=1) indicate cysteine residues more oxidised upon catalase up-
845 regulation, with red symbols designating significance ($p<0.05$), assessed by unpaired two-tailed
846 Student's *t*-test. The total number of unique Cys-containing peptides is indicated in black. **e,** Levels
847 of Nrf2 signalling inferred using a gstD-GFP reporter in da-GS>UAS-cat females treated ±RU for
848 d7 and d28. Western blotting against GFP, catalase and actin, showing 2 biological replicates per
849 condition. **f**, Levels of total glutathione measured in d7 control (UAS-cat/+) and catalase over-
850 expressor females. Data are means ±SEM of n=6 biological replicates, each with n=10 females per
851 sample, analysed by unpaired Student's *t*-test (*, $p>0.01$ head+thorax; ***, $p>0.001$ abdomens).

Figure 4

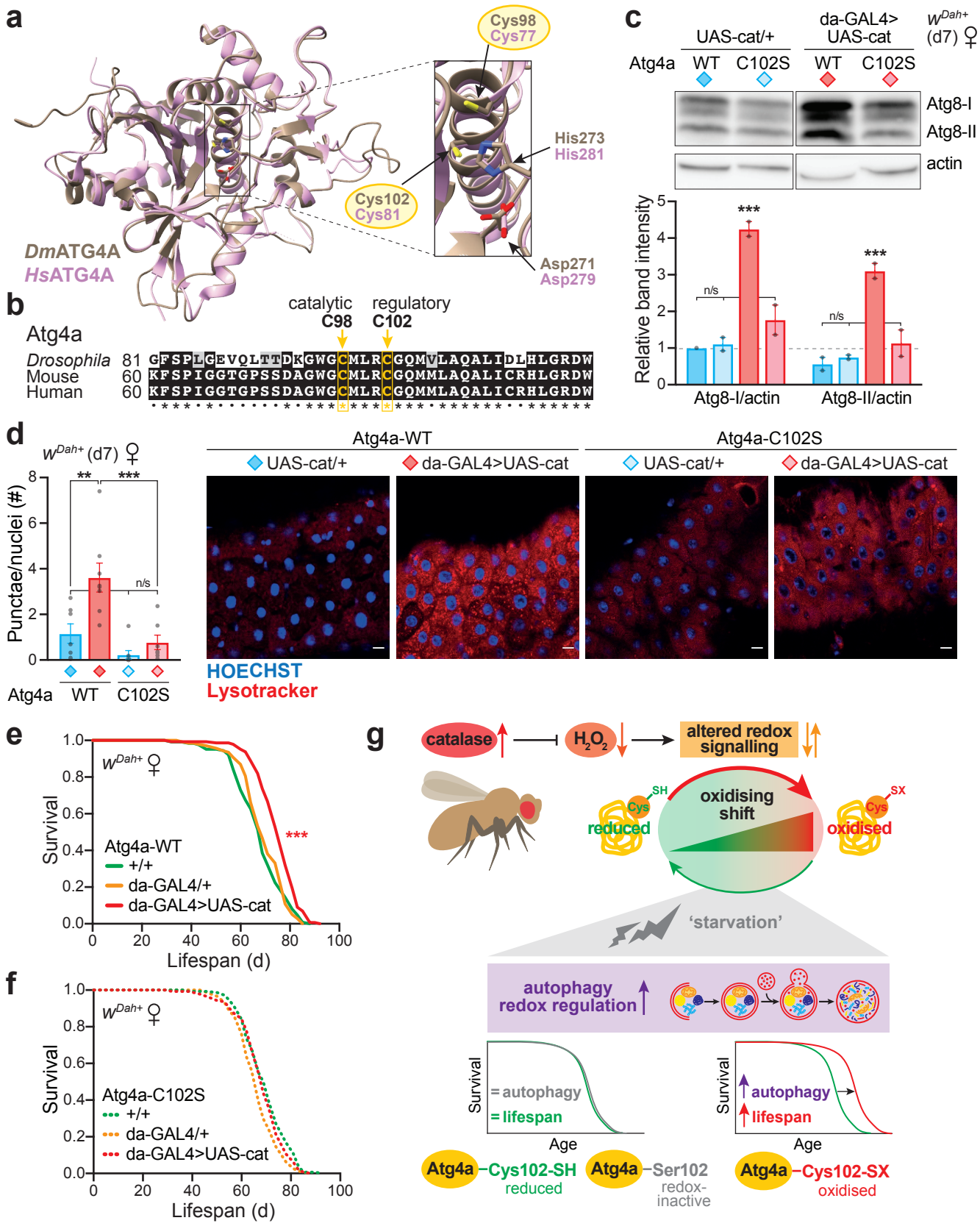
a
Cys98
Cys77
His273
His281
Cys102
Cys81
Asp271
Asp279
DmATG4A
HsATG4A
b
Atg4a
catalytic
C98
regulatory
C102
Drosophila 81 GFSPLGEVQLTTDKGWGCMLRCGQMVLAQALIDLHLGRDW
Mouse 60 KFSPIGGTGPSSDAGWGCMLRCGQMMLAQALICRHLGRDW
Human 60 KFSPIGGTGPSSDAGWGCMLRCGQMMLAQALICRHLGRDW
c
UAS-cat/+
da-GAL4> UAS-cat
wDah+ (d7) ♀
Atg4a WT C102S WT C102S
Atg8-I
Atg8-II
actin
Relative band intensity
***
n/s
Atg8-I/actin
Atg8-II/actin
d
wDah+ (d7) ♀
Punctae/nuclei (#)
**
***
n/s
Atg4a WT C102S
Atg4a-WT
Atg4a-C102S
UAS-cat/+
da-GAL4>UAS-cat
HOECHST
Lysotracker
e
wDah+ ♀
Survival
Atg4a-WT
+/+
da-GAL4/+
da-GAL4>UAS-cat
***
Lifespan (d)
f
wDah+ ♀
Survival
Atg4a-C102S
+/+
da-GAL4/+
da-GAL4>UAS-cat
Lifespan (d)
g
catalase
H2O2
altered redox signalling
reduced
oxidising shift
oxidised
'starvation'
autophagy
redox regulation
Survival
= autophagy
= lifespan
Age
autophagy
lifespan
Age
Atg4a–Cys102-SH
reduced
Atg4a–Ser102
redox-inactive
Atg4a–Cys102-SX
oxidised

852 **Fig. 4 | Redox regulation of autophagy via Atg4a Cys102 extends lifespan. a,** Structural
853 representation of *Drosophila* Atg4a (brown, modelled with Phyre2[73]), superimposed on the crystal
854 structure of human ATG4A (pink, PDB 2P82). Conservation of the catalytic triad and the regulatory
855 cysteine (Cys102/81 in *Drosophila* and human, respectively) are highlighted. Structures were
856 visualised in Chimera X[74]. **b,** Multiple sequence alignment of the Atg4a protein from *Drosophila*
857 with the mouse and human orthologues, showing the catalytic cysteine residue (Cys98 in
858 *Drosophila*) and the redox-regulatory cysteine (Cys102 in *Drosophila*). See Supplementary Fig. 4a
859 for the full sequence. **c-d,** Autophagy induction in response to catalase over-expression was
860 maintained in d7 Atg4a-WT female flies, but abolished in the Atg4a-C102S mutant background. **c,**
861 Autophagy levels assessed by Western blotting against Atg8 (see Supplementary Fig. 4e for the full
862 blot). Quantification of Atg8 levels by densitometry, normalised to actin as a loading control. Data
863 are means ±range of n=2 biological replicates, analysed by two-way ANOVA (Fisher LSD). **d,**
864 LysoTracker Red staining of midguts quantified as the number of punctae relative to HOECHST-
865 stained nuclei (scale bar = 10 µm). Data are means ±SD of n=8 biological replicates, analysed by
866 ANOVA (Tukey; n/s, $p>0.05$; **, $p<0.01$; ***, $p<0.001$). **e-f,** Catalase over-expression extended
867 lifespan in the Atg4a-WT control (**e**), but not in the redox-insensitive Atg4a-C102S knock-in
868 background (**f**). Survival assays (**e**,**f**) were analysed by Log-Rank test (see Supplementary Table 1
869 for full n numbers and p values). n/s, $p>0.05$; ***, $p<0.001$. **g,** Graphical summary: Catalase up-
870 regulation leads to the quenching of H_2O_2 as a second messenger molecule, which results in altered
871 physiological redox signalling. Redox-responsive pathways, such as Nrf2, are not induced, causing
872 an oxiding shift in bulk cysteine thiol redox state, which mimics an internal state of starvation.
873 Autophagy is induced via redox-regulation of Cys102 in Atg4 as a protective response mechanism,
874 which provides health and survival benefits.

875 **Enhancing autophagy by redox regulation extends lifespan in *Drosophila***

876

877

878 ## Supplementary Data

879

880 **Supplementary Figures 1-4**

881

882 **Supplementary Tables 1-5**

883 - Supplementary Table 1: Summary of survival data
884 - Supplementary Table 2: List of cysteine residues identified by OxICAT redox proteomics
885 - Supplementary Table 3: Molecular function and pathway analysis of proteins identified in this
886 study by OxICAT redox proteomics
887 - Supplementary Table 4: Oligonucleotide primers used for cloning and genotyping of the Atg4a-
888 WT and Atg4a-C102S flies
889 - Supplementary Table 5: QPCR primers

Supplementary Figure 1

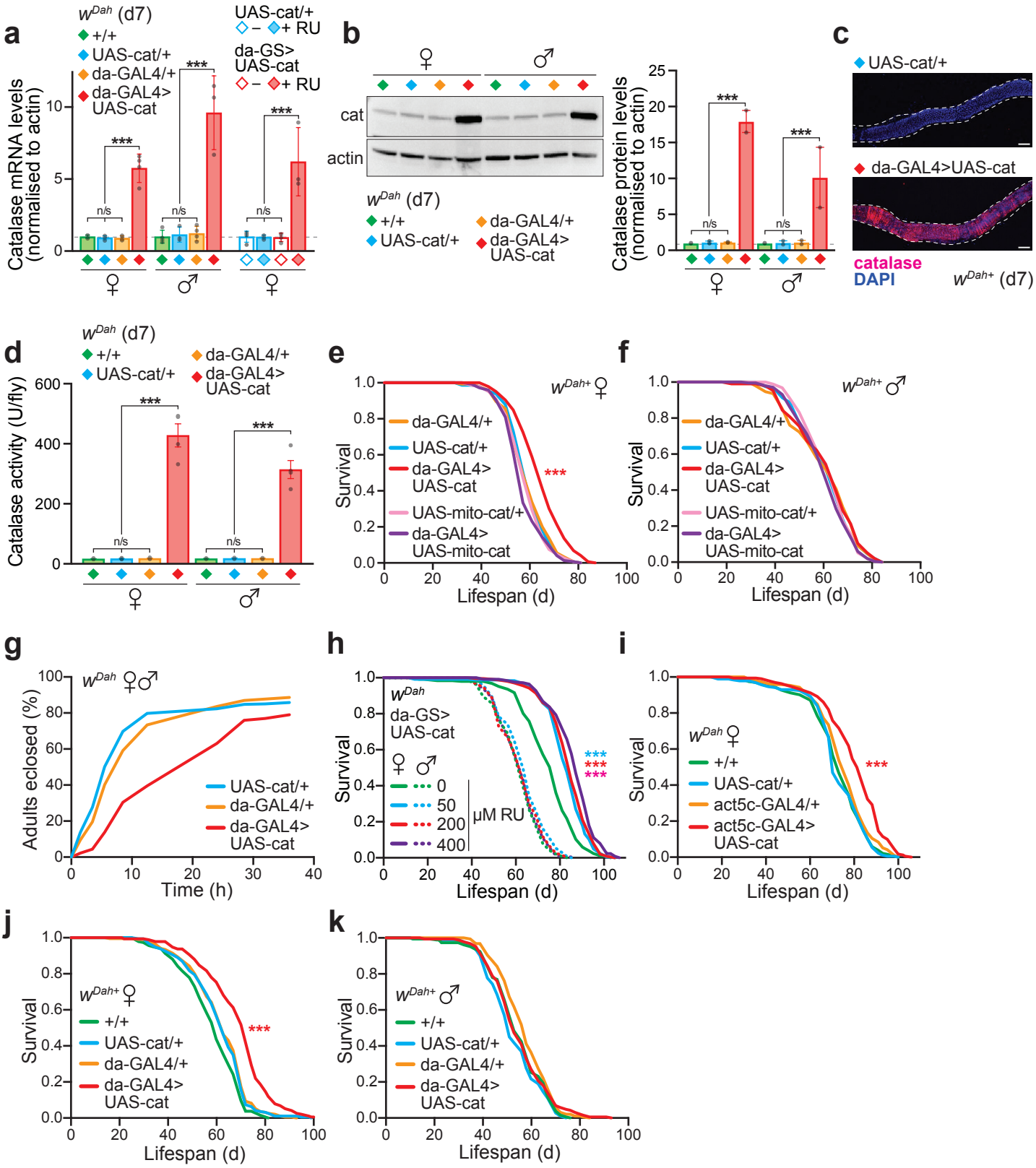

Supplementary Figure 1 (continued)

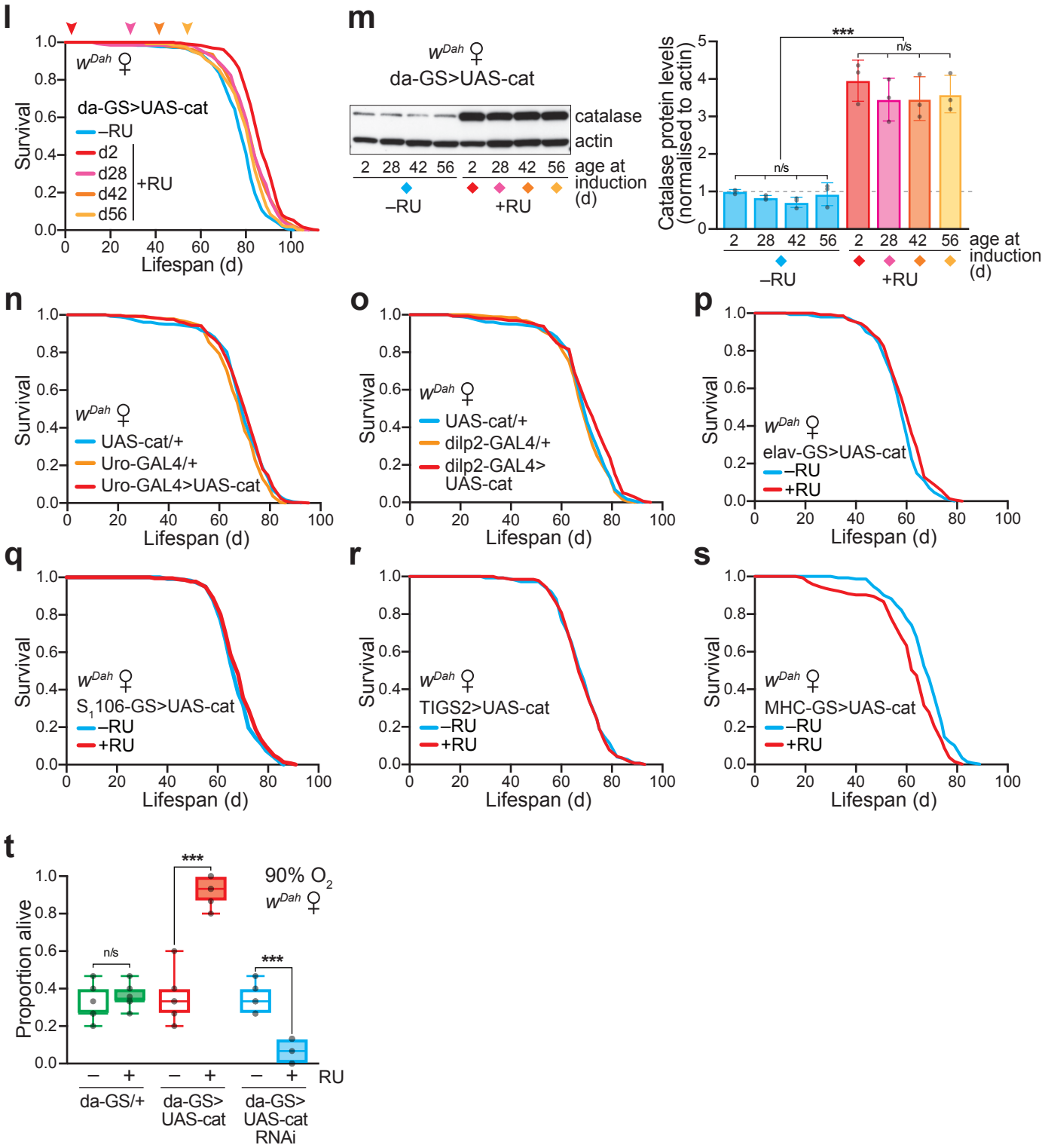

890 **Supplementary Fig. 1 | Ubiquitous catalase up-regulation extends lifespan in flies,**
891 **independently of oxidative stress resistance. a,** Quantification of catalase over-expression by
892 QPCR. Analysis of catalase mRNA levels normalised to actin in constitutive da-GAL4>UAS-cat
893 females and males at d7, and inducible da-GS>UAS-cat +RU females at d9 (=d7 of RU treatment)
894 compared to controls. Data are means ±SD of n=3-4 replicates, each with n=10 whole flies per
895 sample, analysed by one-way ANOVA (Tukey). **b,** Representative Western Blot showing catalase
896 protein abundance in female and male flies at d7. Data are means ±range of n=2 biological replicates,
897 each with n=10 whole flies per sample, analysed by ANOVA (Tukey). **c,** Confocal microscopy of
898 midgut sections showing catalase protein abundance by immunofluorescence (magenta) and nuclei
899 (DAPI, blue) in control (UAS-cat/+) and catalase over-expressor (daGAL4>UAS-cat) females at d7
900 (scale bar = 100 μm). **d,** Catalase enzyme activity in whole female and male flies at d7. Data are
901 means ±SEM of n=4 replicates per condition. n/s ($p<0.05$) by ANOVA (Tukey). **e-f,** Ubiquitous
902 over-expression of mitochondria-targeted catalase (da-GAL>UAS-mito-cat) did not extend lifespan
903 in females ($p>0.05$ *v.* UAS-mito-cat/+ and da-GAL4 controls) or males ($p>0.05$ for all comparisons).
904 Survival assays were performed with n=150 flies per condition. **g,** Development time course.
905 Constitutive ubiquitous catalase over-expression (da-GAL4>UAS-cat) causes a mild developmental
906 delay relative to the UAS-cat/+ and da-GAL4/+ controls. Synchronised L1 larvae (n=500 per
907 genotype) were transferred to SYA vials, and the subsequent eclosion time of adults was recorded.
908 **h,** Dose response of da-GS>UAS-cat lifespan to a range of RU concentrations (0, 50, 200 and
909 400 μM) in both females and males. Survival assays were performed with n=240-255 flies per
910 condition. **i,** Over-expression of catalase with a different ubiquitous driver, actin5c-GAL4, extended
911 lifespan (act5c-GAL4>UAS-cat *v.* UAS-cat/+, $p=3.6x10^{-12}$). Survival assays were performed with
912 n=200 females per condition. **j-k,** Lifespan extension by catalase was independent of *Wolbachia*
913 status. Constitutive catalase over-expression (da-GAL4>UAS-cat) extended the lifespan of female
914 flies in a w^{Dah+} background (c), but not males (d) relative to all controls (+/+, UAS-cat/+ and da-
915 GAL4/+). Survival assays were performed with n=200 flies per condition. **l,** Late onset over-
916 expression of catalase using the inducible GeneSwitch system from either middle-age (d28 and d42)
917 and old-age (d56) extended the lifespan of female flies. Lifespans were performed with n=270 flies
918 per condition. Original survival curves corresponding to Fig. 1e. **m,** Quantification of catalase
919 protein levels by Western blotting with age and upon late-onset induction (see Fig. 1e). Flies (da-
920 GS>UAS-cat) were sampled 7 d after the indicated age of RU treatment initiation. Left, typical
921 Western blot probed against catalase with actin as a loading control. Right, quantification by
922 densitometry. Data are means ±SD of n=3 biological replicates per time point, each with n=5 flies
923 per sample, analysed by one-way ANOVA (Tukey). **n-s,** Tissue-specific over-expression of
924 catalase: **n,** in the Malphigian tubules (the fly equivalent of the kidney) driven by Uro-GAL4 (n=300

925 females per condition, except n=285 for UAS-cat/+); **o,** in the insulin producing cells (IPCs) driven
926 by dilp2-GAL4 (n=300 females per condition, except n=285 for UAS-cat/+); **p,** pan-neuronal driven
927 by elav-GS (n=150 females per condition); **q,** in the intestine and fat body (the fly equivalent of the
928 liver/adipose tissue) driven by $S_1$106-GS (n=225 females per condition); **r,** in the gut driven by
929 TIGS2 (n=150 females per condition); **s,** pan-muscular driven by the myosin heavy chain driver
930 MHC-GS (n=150 females per condition). **t,** Catalase RNAi flies were sensitive to hyperoxia stress
931 relative to controls. Incubation at 90% O_2 was initiated at d9 (= d7 of RU treatment), and the fraction
932 alive scored after 4 d. Data are presented as box-and-whisker plots (min/max error bars) with n=7
933 vials per condition (each with n=15 flies), analysed by one-way ANOVA (Tukey) (da-GS/+ ±RU,
934 p=0.939; da-GS>UAS-cat ±RU, $p<1x10^{-15}$; da-GS>UAS-catRNAi ±RU, $p=7.01x10^{-6}$). All survival
935 assays (**e**,**f**,**h**,**i**,**j**,**k**,**l**,**m,n,o,p,q,r,s**) were analysed by Log-Rank test (see Supplementary Table 1 for
936 full n numbers and p values). n/s, p>0.05; ***, p<0.001.

Supplementary Figure 2

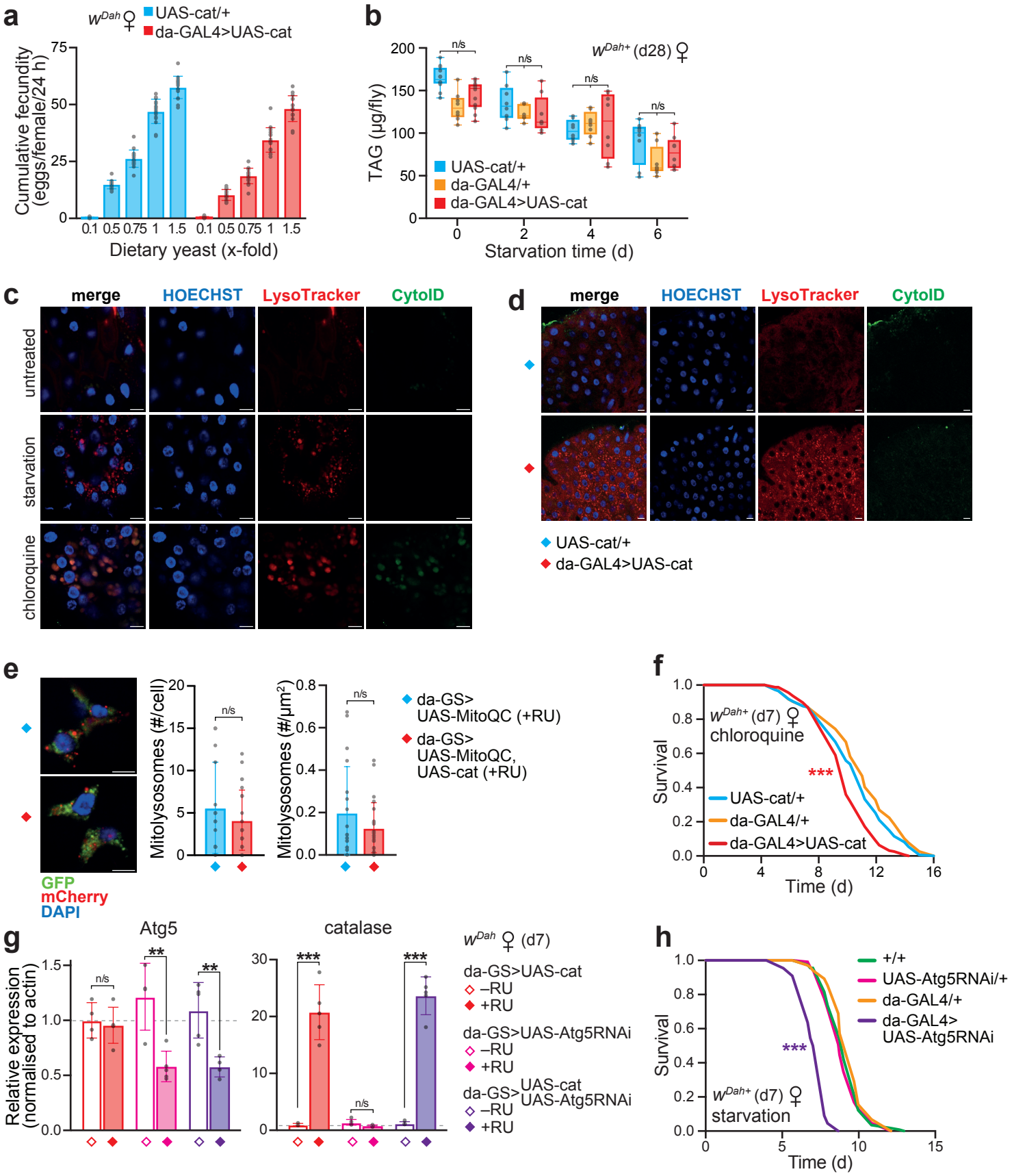

937 **Supplementary Fig. 2 | Catalase lifespan extension requires autophagy. a,** Response of egg
938 laying to DR. Cumulative fecundity (egg laying at d7 + d14 + d21) for each genotype at a range of
939 dietary yeast concentrations, with 1x corresponding to standard SYA food. Data are means ±SD of
940 n=16 vials per genotype, each set up with n=10 females per vial, analysed by one-way ANOVA
941 (Tukey, p<0.001 for all comparisons within each genotype). **b,** Whole body TAG levels in females
942 assayed at d28 (t=0) and in response to a starvation timecourse. Data are presented as box-and-
943 whisker plots (min/max error bars) of n=4-12 replicates per genotype, each with n=5 females per
944 sample, analysed by ANOVA (n/s, p>0.05). **c-d,** Confocal imaging of d7 female midguts stained
945 with LysoTracker Red and CytoID, as indicators of autophagolysosome formation and autophagic
946 flux respectively (scale bar = 10 µm). **c,** Starvation (48 h) increased LytoTracker punctae in control
947 (UAS-cat/+) females, while treatment with the inhibitor chloroquine (10 mM in SYA, 48 h) blocked
948 autophagic flux, leading to increased CytoID signal. **d,** Autophagy is induced in catalase over-
949 expressors (da-GAL4>UAS-cat) compared to controls (UAS-cat/+), without affecting flux. Images
950 of individual channels, corresponding to Fig. 2f. **e**, Catalase up-regulation does not impact
951 mitophagy, as inferred from the mito-QC reporter. Confocal images of dissected midguts showing
952 mitolysosome punctae (scale bar = 5 µm). Data are the means ±SD of n=8-10 counts per genotype,
953 analysed by unpaired Student's *t*-test (p>0.05). **f,** Catalase over-expressor females (da-GAL4>UAS-
954 cat) were sensitive to treatment with the autophagy inhibitor chloroquine (10 mM in sucrose/agar
955 medium) relative to UAS-cat/+ and da-GAL4/+ controls ($p=2.6x10^{-5}$ and $p=3.5x10^{-9}$, respectively).
956 Assays were performed at d7 with n=160 flies per condition. **g,** QPCR quantification of Atg5 and
957 catalase levels upon Atg5 RNAi and catalase over-expression, normalised to actin. Female flies were
958 sampled at d9 (=d7 of RU treatment), using RNA extracted from head and thorax tissue. Data are
959 means ±SD of n=4-5 replicates per condition, each with n=10 flies per sample, analysed by one-way
960 ANOVA (Tukey). **h,** Ubiquitous Atg5 RNAi results in sensitivity to starvation stress. The assay was
961 set up at d7 with n=20-140 flies per genotype, using the GAL4 driver (rather than GeneSwitch) to
962 maintain Atg5-RNAi during starvation stress where RU is not present (p<0.001 for da-GAL4>UAS-
963 Atg5RNAi compared to all controls). All survival assays (**f,g**) were analysed by Log-Rank test (see
964 Supplementary Table 1 for full n numbers and p values). n/s, p>0.05; ***, p<0.001.

Supplementary Figure 3

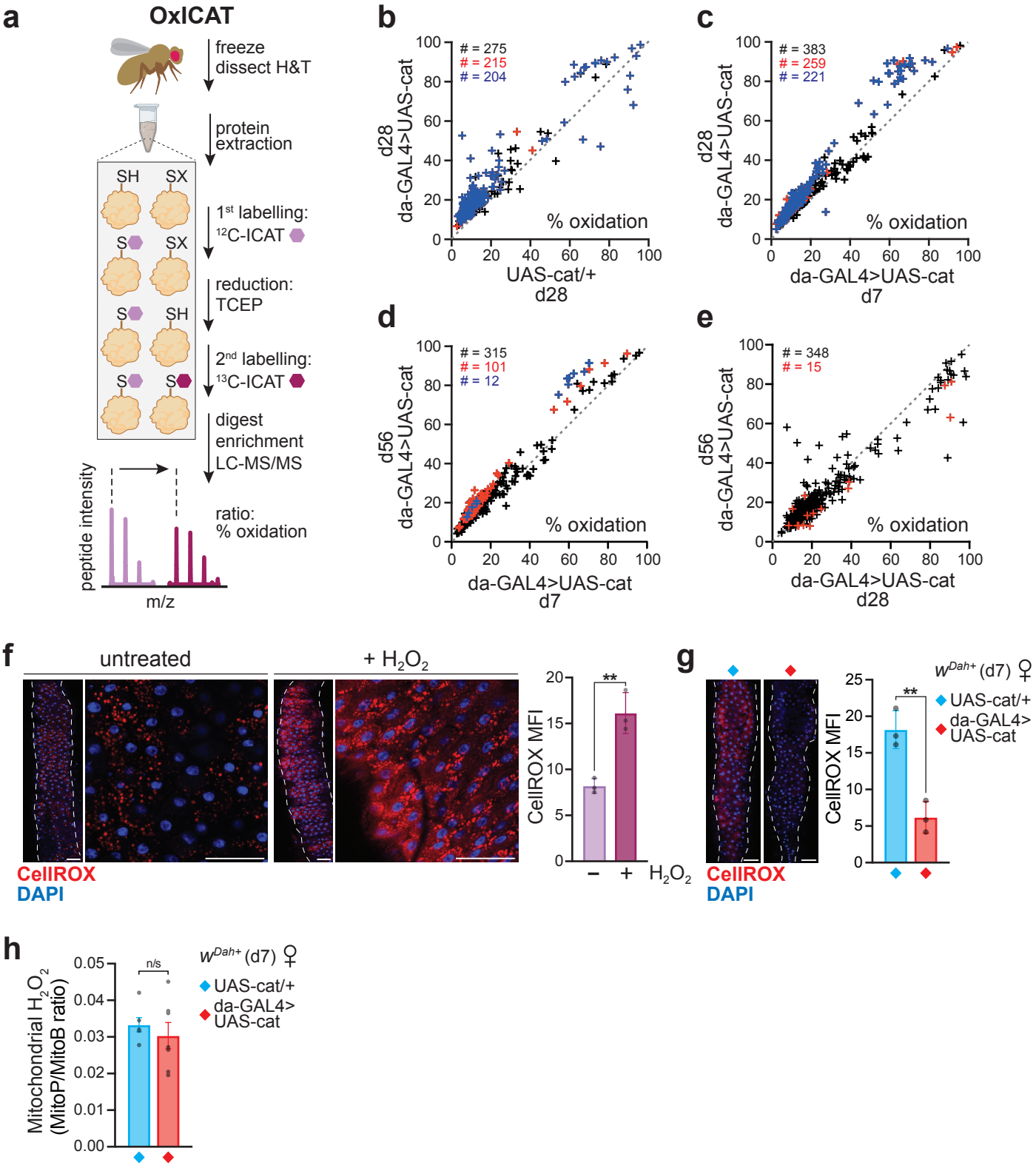

965 **Supplementary Fig. 3 | Catalase flies undergo an oxidising shift in global thiol redox state. a,**
966 Scheme of the OxICAT workflow for unbiased redox proteomics. Cysteines are differentially
967 labelled according to redox status using light and heavy ICAT probes. **b-e,** OxICAT analysis.
968 Oxidation state of Cys residues present, comparing control (UAS-cat/+) *v.* catalase over-expressor
969 (da-GAL4>UAS-cat) females at d28 (**a**), d7 *v.* d28 catalase over-expressors (**b**), d7 *v.* d56 catalase
970 over-expressors (**c**), and d28 *v.* d56 catalase over-expressors (**d**). Data points above or below the
971 diagonal dotted line (slope=1) indicate a change in Cys redox state, with red symbols designating
972 low stringency significance ($p<0.05$, assessed by unpaired two-tailed Student's *t*-test) and blue
973 symbols high stringency significance (Benjamini-Hochberg test). The total number of unique Cys-
974 containing peptides is indicated in black. **f-g,** H_2O_2 levels inferred from the fluorescent redox-
975 reactive probe CellROX assessed by confocal microscopy of dissected midguts (scale bar = 50 µm).
976 Data are means ±SD of n=3 samples per condition. **f,** Response of control tissue incubated $\pm H_2O_2$
977 as a positive control for the assay (p=0.0044). **g,** CellROX staining of catalase up-regulated guts,
978 showing decreased signal compared to control (p=0.003564). **h,** Mitochondrial H_2O_2 levels
979 quantified using the MitoB probe, showing similar levels in control and catalase up-regulated flies.
980 Data are means ±SEM of n=6-7 samples per genotype (p=0.5045). Data (**f-h**) are for d7 females,
981 analysed by unpaired 2-tailed Student's *t*-test (n/s, $p>0.05$; **, $p<0.01$).

Supplementary Figure 4

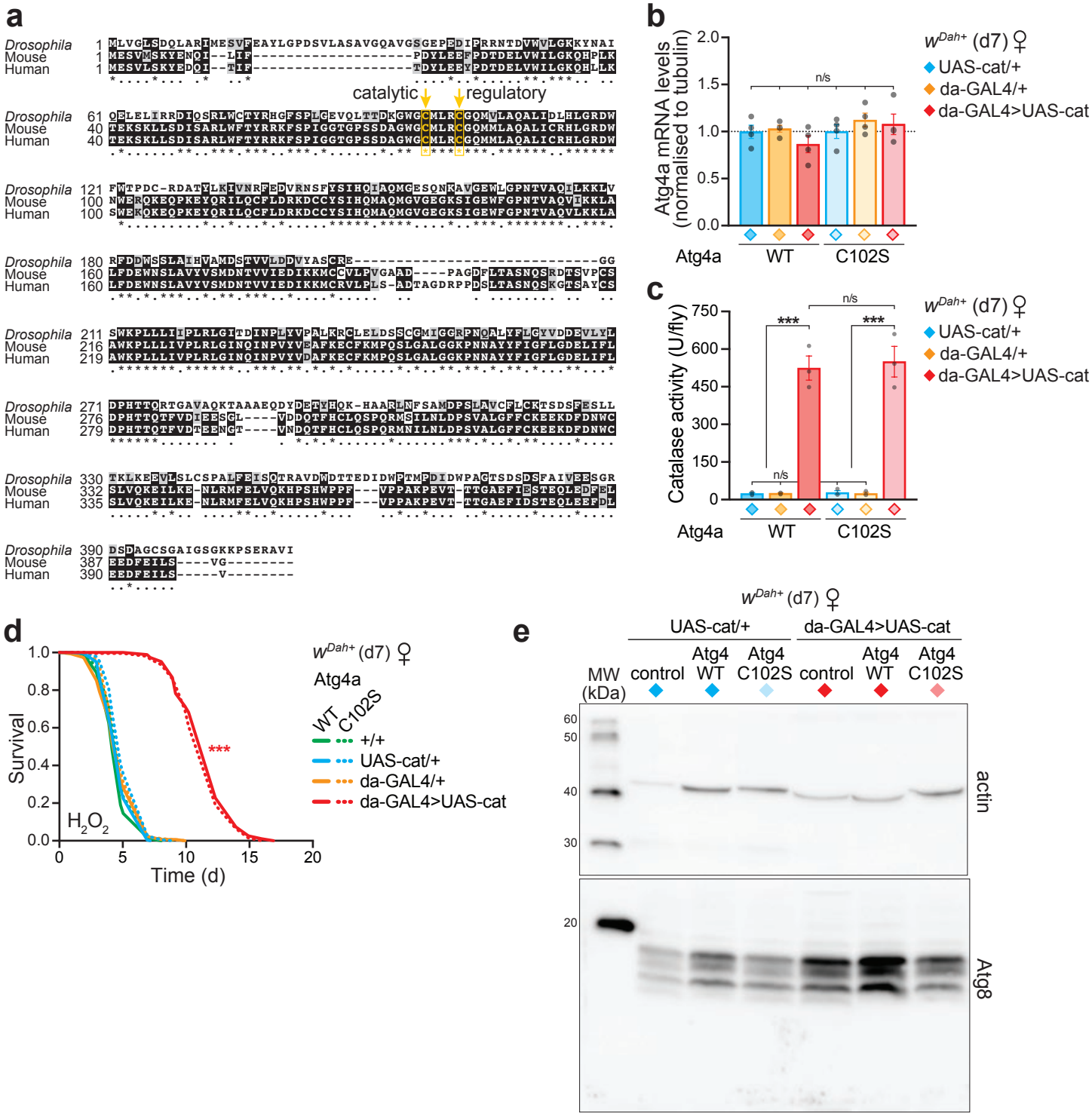

Supplementary Figure 4 (continued)

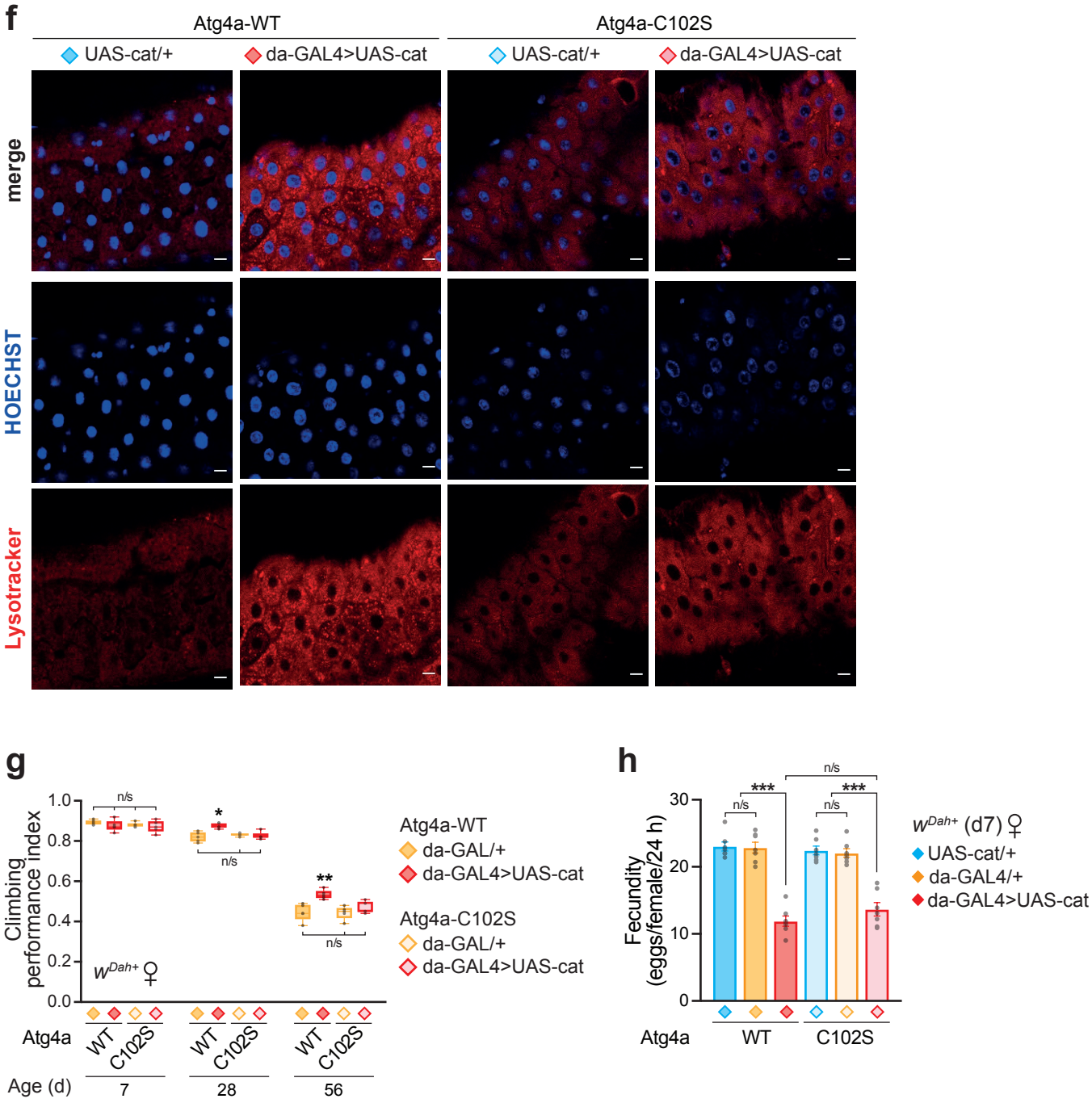

982 **Supplementary Fig. 4 | Redox regulation of autophagy via Atg4 Cys102 extends lifespan. a,**
983 Multiple sequence alignment of Atg4a from *Drosophila* with the mouse and human orthologues
984 (UniProt IDs # Q9VPW2, Q8C9S8 and Q8WYN0, respectively) performed in T-Coffee
985 (www.tcoffee.org). **b,** Atg4a expression levels were not affected by the C102S mutation or catalase
986 over-expression, as assessed by QPRC, normalised to tubulin. Data are the means ±SD of n=4
987 replicates, analysed by ANOVA (Tukey, p>0.05 for all comparisons). **c,** The Atg4a-C102S mutation
988 did not change levels of catalase up-regulation, as measured by enzyme activity. Data are the means
989 ±SD of n=3 replicates, analysed by ANOVA (Tukey, *** p<0.001, n/s p>0.05). **d,** H_2O_2 stress
990 resistance was comparable between Atg4a-WT flies and Atg4a-C102S knock-in mutants, both under
991 control conditions and upon catalase up-regulation. H_2O_2 treatment (5% v/v in sucrose/agar
992 medium) was initiated at d7, with n=160 females per genotype. Survival assays were analysed by
993 Log-Rank test (see Supplementary Table 1 for full n numbers and p values). n/s, p>0.05, ***,
994 p<0.001. **e,** Full Western blots corresponding to data in Figs. 2g and 4c. After transfer, the upper
995 portion of the membrane was probed for actin as a loading control, while the lower portion of the
996 membrane was probed against Atg8. **f,** Autophagy induction in response to catalase over-expression
997 was maintained in d7 Atg4a-WT female flies, but abolished in the Atg4a-C102S mutant background,
998 as assessed by LysoTracker Red staining of midguts (scale bar = 10 μm). Images of individual
999 channels, corresponding to Fig. 4d. **g,** Climbing assay of control (da-GAL/+) and catalase over-
1000 expressors (da-GAL>UAS-cat) in Atg4a-WT and Atg4a-C102S backgrounds. Data are presented as
1001 box-and-whisker plots (min/max error bars) of n=5 replicates per condition, each with n=15 flies
1002 per sample, analysed by ANOVA (n/s, p>0.05; *, p<0.05; **, p<0.01). **h,** The Atg4a-C102S
1003 mutation does not alter egg laying upon catalase up-regulation compared to the control Atg4a-WT
1004 background in d7 females. Data are the means ±SEM of n=7 vials per genotype, each set up with
1005 n=15 females per vial, analysed by one-way ANOVA (Tukey, n/s, p>0.05; ***, p<0.001).